Crustal Structure and Tectonic Evolution of the Southern Baltic Sea Interpreted from Seismic, Gravity and Magnetic Data

M. Ponikowska[1], S. M. Stovba[1,2], S. Mazur[1], M. Malinowski[3,4], P. Krzywiec[1], Q. Nguyen[3], and C. Hübscher[5]

[1] Institute of Geological Sciences, Polish Academy of Sciences, Warsaw, Poland

[2] S.I. Subbotin Institute of Geophysics, National Academy of Sciences of Ukraine, Kyiv, Ukraine

[3] Institute of Geophysics, Polish Academy of Sciences, Warszawa, Poland

[4] Geological Survey of Finland, Espoo, Finland

[5] Institute of Geophysics, University of Hamburg, Hamburg, Germany

Corresponding author: Małgorzata Ponikowska (m.ponikowska@ingpan.krakow.pl)

Key Points:

- The southern Baltic Sea is underlain by thick crust of the East European Craton with a Moho depth in the range of 38-42 km.
- The Sorgenfrei-Tornquist and Teisseyre-Tornquist Zones represent 80-90 km wide zones of localized Late Cretaceous-Paleocene inversion.
- Inversion zones include a system of thrusts and backthrusts penetrating the entire crust, and forming a crustal-scale pop-up structure.

Abstract

The Teisseyre-Tornquist Zone (TTZ) is the longest pre-Alpine tectonic lineament in Europe. Its nature and structural evolution are controversially debated. In this study, we show its structural evolution beneath the southern Baltic Sea both on crustal and basin scale by using three seismic reflection profiles combined with 2-D potential field data. The results demonstrate that the southern Baltic Sea is underlain by a thick crust of the East European Craton (EEC) with a Moho depth in the range of 38-42 km. The overall crustal architecture is shaped by three phases of localized crustal stretching in early Paleozoic, Devonian-Carboniferous, and Permian-Mesozoic. The most spectacular feature of the southern Baltic Sea are zones of thick-skinned compressional deformation produced by Alpine inversion along the TTZ and Sorgenfrei-Tornquist Zone (STZ). Both zones include a system of thrusts and back thrusts penetrating the entire crust in an 80-90 km wide inversion zone superimposed on the EEC crust and its sedimentary cover. ENE-vergent thrusts are traced from the top of the Cretaceous down to the Moho and they are accompanied by back thrusts of opposite vergence, also reaching the Moho. Inversion tectonics resulted in the uplift of a block of cratonic crust as a pop-up structure, bounded by thrusts and back thrusts, and the displacement of the Moho within the STZ and TTZ. The similar mechanism of intra-cratonic inversion was recognized for the Dnieper-Donbas Basin in eastern Ukraine, and it may be characteristic of rigid cratons, where deformation is localized in a few preexisting zones of weakness.

1 Introduction

The transition zone between the East European Craton (EEC) and the Paleozoic Platform of Western Europe (Fig. 1) is still a matter of discussion despite numerous geophysical data that have been so far acquired (e.g., Berthelsen, 1998; Pharaoh, 1999; Thybo, 2001; Bayer et al., 2002). This is primarily because of a thick cover (5-14 km; Maystrenko and Scheck-Wenderoth, 2013; Mazur et al., 2021) of Paleozoic and Mesozoic sediments obscuring the original crustal architecture. These sediments mask a suture zone between East Avalonia in the SW and Baltica in the NE, the character of which has been variously interpreted over the past decades (e.g., Tanner and Meissner, 1996; Berthelsen, 1998; Bayer et al. 2002; Dadlez et al., 2005; Mazur et al., 2015, 2016; Smit et al., 2016). Therefore, the transition between old Precambrian Europe in the east and younger mobile Europe in the west is not fully understood. Consequently, several important questions regarding segmentation of Rodinia, amalgamation of Pangea and the nature of basement underlying the Permian-Mesozoic basin of NW Europe remains still open.

A lower Paleozoic succession, including gas-prone Silurian shales, is intensely folded and thrust SW of the Caledonian Deformation Front (CDF), crossing Denmark and the southern Baltic Sea to northern Poland (Fig. 1; Katzung et al., 1993; Lassen et al., 2001; Krawczyk et al., 2002). Furthermore, the area was affected by widespread extensional tectonics in the early Carboniferous (Smit et al., 2018; Krzywiec et al., 2022) and Permian-Mesozoic (e.g., Maystrenko et al., 2008). Finally, the Late Cretaceous-early Paleogene basin inversion vastly modified the pre-existing tectonic features (e.g., Krzywiec et al., 2003; Mazur et al., 2005; Al Hseinat and Hübscher, 2017; Kley, 2018; Krzywiec et al., 2022; Stachowska and Krzywiec, 2023). These superimposed tectonic events produced a complex structural pattern (Tab. 1) that impedes understanding of the crustal structure at the transition from the thick crust of the EEC to the thinner crust of the Paleozoic Platform farther SW.

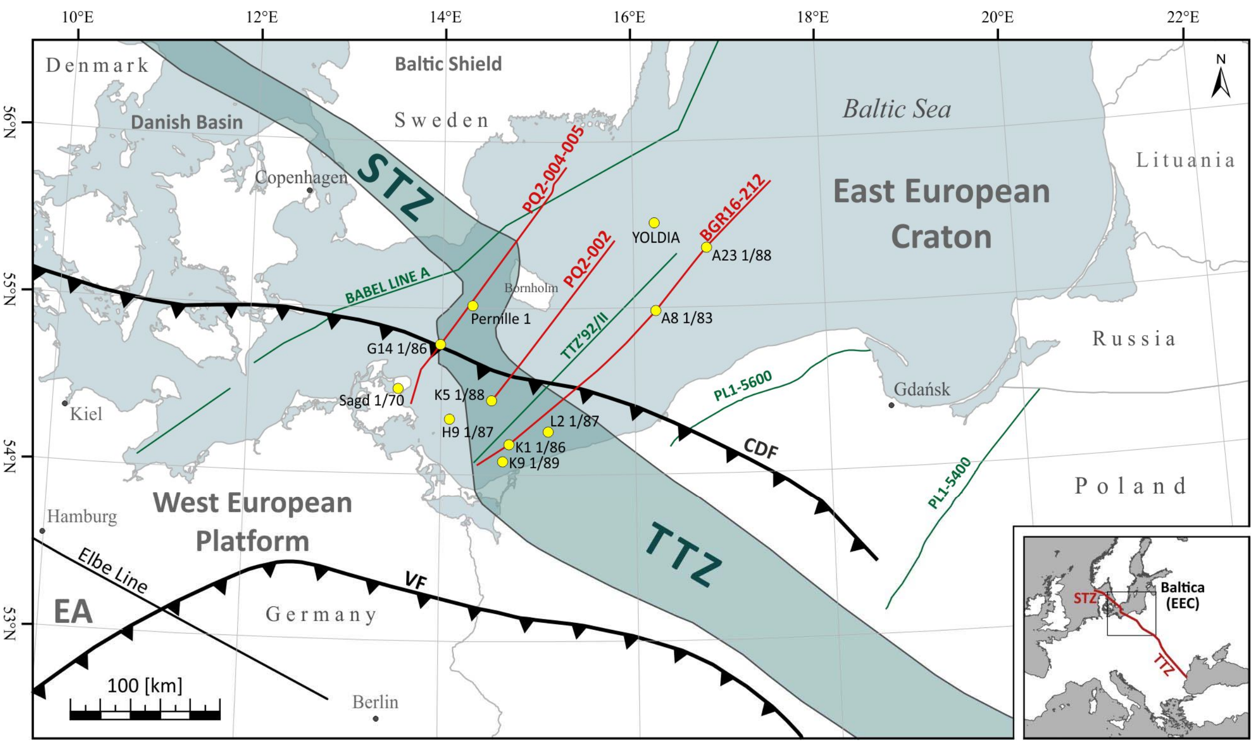

Figure 1. Location of the BGR16-212, DEKORP-PQ (PQ2-004-005 and PQ2-002) and other seismic profiles: BABEL A (BABEL Working Group, 1991, 1993), TTZ'92/II (Makris and Wang, 1994) and PolandSPAN™ PL-5400 and PL-5600 (Mazur et al., 2015, 2016b) on the background of a simplified tectonic map of the transition zone from the East European Craton to West European Platform. Yellow points refer to the location of offshore boreholes (Erlström et al., 1997; Sopher et al., 2016; Central Geological Database, 2019). Location of the Teisseyre-Tornquist Zone and Sorgenfrei-Tornquist Zones after Grad et al. (2002). Abbreviations: CDF – Caledonian Deformation Front; EA – East Avalonia; STZ – Sorgenfrei-Tornquist Zone; TTZ – Teisseyre-Tornquist Zone; VF – Variscan Front. The coordinate system of this and next figures is WGS 1984 UTM Zone 33 N.

Within the Baltica-Avalonia transition zone, the southern Baltic Sea is a peculiar area, where the Sorgenfrei-Tornquist Zone (STZ), extending from Bornholm across the Baltic Sea and northern Denmark into the North Sea, connects to the Teisseyre-Tornquist Zone (TTZ) that continues from the Polish coast to the Black Sea (Figs. 1, 2). However, the basement SW of the STZ is still similar to that of the EEC (e.g., Berthelsen, 1992) so the STZ is interpreted as a major intra-cratonic feature. In contrast, the TTZ is sometimes believed to be an actual edge of the EEC (e.g., Dadlez et al., 2005; Narkiewicz et al., 2015) based on the dissimilar crustal velocity structure that was revealed by the deep wide-angle reflection/refraction (WARR) data on both sides of the TTZ (c.f. Guterch and Grad, 2006 for overview). Therefore, a link between the STZ and TTZ, commonly postulated across the southern Baltic Sea in numerous papers (e.g., Pharaoh 1999; Meissner and Krawczyk, 1999; Thybo, 2000; Pharaoh et al., 2006; Guterch et al., 2010), requires further testing in search for a consistent interpretation of both lithospheric features.

Table 1. Synopsis of tectonic events in the area of the southern Baltic Sea.

Timing	Tectonic regime	Effects	References
Cenozoic	E-W renewed extension thermal subsidence	Deposition of a thin and patchy sedimentary cover	Maystrenko et al. (2005), Ahlrichs et al. (2022)
Late Cretaceous-earliest Paleogene	Tectonic inversion of the Permian-Mesozoic basin	Formation of folds and pop-up structures, subsidence at marginal troughs	Deeks and Thomas (1995), Krzywiec et al. (2003), Mazur et al. (2005), Krzywiec (2006b), Krzywiec et al. (2022), Pan et al. (2022), this study
Late Permian-Cretaceous	Thermal subsidence punctuated by pulses of renewed tectonic extension	Growth of the Polish, NE German and Danish Basins	Dadlez et al. (1995), Dadlez (2003), Krzywiec (2006a), Mazur et al. (2005), this study
Early Permian	Continental rifting	Formation of the MPT, thinning of the EEC margin	McCann et al. (2006), Scheck-Wenderoth et al. (2008), Mazur et al. (2021)
Late Carboniferous	Variscan orogeny	Inversion of late Palaeozoic sedimentary basins; pre-Permian unconformity	Erlström et al. (1997), Krzywiec et al. (2022), this study
Devonian-early Carboniferous	Post-orogenic collapse, continental rifting, thermal subsidence	Formation of tectonic grabens and half-grabens SW of the STZ and TTZ	Smit et al. (2018), Krzywiec et al. (2022), this study
Ordovician-Silurian	Caledonian orogeny – thick- (Rügen) to thin-skinned (onshore Poland) thrusting onto the Baltica margin	Formation of the Caledonian orogenic wedge and foreland basin	Katzung et al. (1993), Dallmeyer et al. (1999), Mazur et al. (2016), this study
Cambrian-Early Ordovician	Passive margin thermal subsidence	Deposition on the passive margin of Baltica	Poprawa et al. (1999), Poprawa (2019)
Ediacaran	Break-up of Rodnia, stretching of the Baltica margin	Initiation of the TTZ and STZ(?), thinning of the present EEC margin	Mikołajczak et al. (2019), Mazur et al. (2021)

We have conducted a comprehensive analysis involving gravity and magnetic data collected in the South Baltic Sea. Our approach is complemented by a thorough reevaluation of the DEKORP-BASIN’96 deep reflection seismic profiles, originally interpreted by the DEKORP-BASIN Research Group (1998). Additionally, we have meticulously interpreted recent seismic data obtained from the BalTec project (Hübscher et al., 2017), which traverse the STZ and TTZ in an ENE-WSW direction, confirming their precise location, characteristics, and evolutionary traits (Figs. 1, 2). We have also constructed grids representing pivotal seismic horizons that outline the crustal architecture in the southern Baltic Sea region. Our investigation aims to discern whether the TTZ truly demarcates the craton's boundary or, akin to the STZ, signifies an intra-cratonic aspect. Furthermore, we address the interplay between the inversion structures emerging in the Late Cretaceous time and the pre-existing tectonic attributes within the South Baltic Sea. Ultimately, we propose an innovative interpretation concerning the profound crustal configuration in the Baltic sector of the transitional zone connecting former Baltica and East Avalonia.

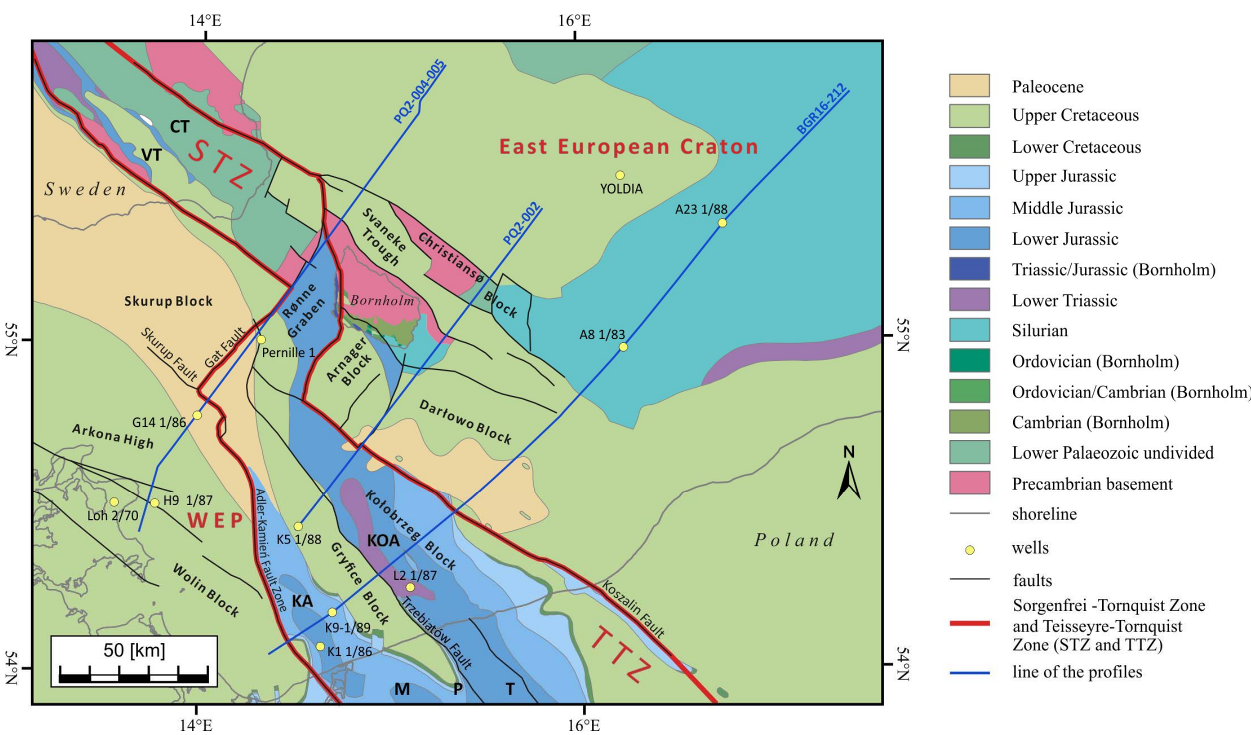

Figure 2. Geological map of the southern Baltic Sea without post-Paleocene sediments after Kramarska et al. (1999), Schlüter et al. (1998), Sopher et al. (2016) and Pre-Quaternary map of Bornholm (Hansen and Poulsen, 1977). Position of main faults and tectonic blocks as well as the Teisseyre-Tornquist and Sorgenfrei-Tornquist Zones are adapted from Seidel et al. (2018). The studied seismic profiles are shown as blue lines. Abbreviations: CT – Colonus Trough; KA – Kamień Anticline; KOA – Kołobrzeg Anticline; MPT – Mid-Polish Trough; STZ – Sorgenfrei-Tornquist Zone; TTZ – Teisseyre-Tornquist Zone; VT – Vomb Trough; WEP – West European Platform.

2 Geological setting and previous geophysical studies

The southern Baltic Sea extends over the boundary of two major geological domains – the East European Precambrian Platform in the NE and the Paleozoic Platform of Western Europe in the SW (Fig. 1). The former domain is composed of the EEC basement and a little deformed Proterozoic-Phanerozoic sedimentary cover, while the latter includes early Paleozoic non- to low-grade metamorphic basement (the North German-Polish Caledonides) and a Devonian-Cenozoic sedimentary pile (e.g., Berthelsen, 1992; Pharaoh 1999). A matter of discussion remains, whether the NE part of the Paleozoic Platform is underlain by an attenuated margin of the EEC (Berthelsen, 1992, 1998; Tanner and Meissner, 1996; Pharaoh, 1999; Lassen et al., 2001; Bayer et al., 2002; Krawczyk et al., 2002; Mazur et al., 2015, 2016a, b) or the EEC is sharply truncated along the TTZ (Franke, 1994; Dadlez et al., 2005; Narkiewicz et al., 2015; Narkiewicz and Petecki, 2017). This is due to the fact that the location and structure of the suture between Baltica and East Avalonia is obscured by thick Paleozoic-Cenozoic sediments and insufficiently imaged by seismic data. Nevertheless, most of previous studies suggest that the Precambrian EEC (Baltica) crust continues SE-ward underneath the North German-Polish Caledonides and the NE German Basin (DEKORP-BASIN Research Group, 1999; Gossler et al., 1999; Krawczyk et al., 1999) and it may extend as far as the Elbe Lineament (Berthelsen, 1992; Tanner and Meissner, 1996; Bayer et al., 2002; Mazur et al., 2015, 2016b; Smit et al., 2016). This view has been challenged by Dadlez et al. (2005) postulating that the TTZ represents a tectonic strike-slip suture, coincident with a transverse margin of Baltica, where proximal Batica-derived terranes, displaced along the TTZ, were docked in the Ordovician-early Silurian. However, this hypothesis fails to explain why the CDF diverges from the TTZ in southern Baltic Sea (Fig. 1) and why the TTZ is linked in the vicinity of Bornholm to the STZ. Moreover, the interpretation by Dadlez et al. (2005) is in contrast to a thin-skinned character of the Caledonian fold-and-thrust belt onshore NW Poland (Mazur et al., 2016b). Given the contrasting interpretations mentioned above, the southern Baltic Sea is a key area for resolving the character of the TTZ and its relationship to the STZ and Caledonian orogen.

The southern Baltic Sea is characterized by a mosaic of various geological blocks separated by several fault zones formed throughout the Phanerozoic (Tab. 1; Figs. 2, 3; Liboriussen et al., 1987; Berthelsen, 1992; Vejbæk et al., 1994; Pharaoh, 1999; Thybo, 2000; van Wees et al., 2000) and it is often defined as the Trans-European Suture Zone (TESZ; Pharaoh, 1999). Major, often deeply rooted faults (Fig. 3) governed subsidence and uplift of major crustal blocks during several tectonic phases in Paleozoic, Mesozoic and, locally, also Cenozoic (Tab. 1; Dadlez, 1993; Erlström et al., 1997; Krzywiec et al., 2003; Al Hseinat and Hübscher, 2017; Ahlrichs et al., 2022; 2023). The most prominent tectonic features are the NW–SE trending STZ and TTZ, crossing the southern Baltic Sea north and south of Bornholm, respectively (Figs. 1, 2). The STZ represents a major lithospheric structure, separating the Danish Basin from the Baltic Shield (Fig. 1), with a significant increase in lithosphere thickness from the SW to NE (Babuška and Plomerová, 2004; Hansen et al., 2007). This zone coincides with a pronounced change in crustal thickness with a Moho depth increasing from 30-32 km to 35-48 km beneath the Danish

Basin and Baltic Shield, respectively (e.g., Thybo 2001; Cotte et al., 2002). The TTZ is the longest European tectonic and geophysical lineament extending from the Baltic Sea in the NW to the Black Sea in the SE (Fig. 1; Pharaoh, 1999). This tectonic feature delineates a transition between the thick crust of the EEC in the NE and the thinner crust of the Paleozoic Platform in the SW. The TTZ is an up to 50 km wide zone corresponding to a change in a Moho depth from 42 to 49 km beneath the EEC to 31–38 km farther SW below the Paleozoic Platform (Guterch and Grad, 2006; Guterch et al., 2010; Mazur et al., 2021). This zone of Moho uplift is associated with a slope of the Precambrian basement descending c. 10–12 km SW-ward underneath extensive Paleozoic and Mesozoic sedimentary successions (Mazur et al., 2015, 2021; Grad and Polkowski, 2016; Mikołajczak et al., 2019). The TTZ was recently interpreted as a necking zone related to break-up of the Rodinia supercontinent in the Ediacaran and coeval stretching of a passive continental margin of Baltica (Mazur et al., 2016a, 2021; Mikołajczak et al., 2019). However, early Permian continental rifting may have also contributed to crustal thinning across the TTZ (Mazur et al., 2021; Jóźwiak et al., 2022). This view follows an earlier interpretation by Berthelsen (1998), who considered the TTZ a feature entirely developed due to the earliest Permian continental rifting in accordance with the Wernicke simple-shear model (Wernicke, 1985).

A crustal keel underneath the TTZ was postulated in NW and central Poland, based on potential field modelling along the PolandSPAN™ seismic profiles (Mazur et al., 2015, 2016). In central Poland, the TTZ is overlain by almost undisturbed lower Paleozoic sediments, the situation precluding a role of the Caledonian orogeny in creating the crustal keel (Mazur et al., 2015). Furthermore, the PolandSPAN™ seismic profiles show smooth top of basement plunging to the WSW across the TTZ, the geometry excluding a Phanerozoic suture of two basement terranes (Mazur et al., 2015, 2016). In the southern Baltic Sea, a crustal keel was imaged by BABEL profile A, which crossed the STZ NW of Bornholm (BABEL Working Group, 1991, 1993; Thybo et al., 1994). A similar feature, i.e., deepening of the Moho below the TTZ, was also recognized by the TTZ'92/II profile crossing the southern Baltic Sea between Polish coast and Bornholm (Makris and Wang, 1994). Consequently, both the STZ and TTZ were interpreted as a feature formed by Late Cretaceous–early Cenozoic inversion tectonics (BABEL Working Group, 1993; Makris and Wang, 1994; Thybo et al., 1994). The keel underneath the STZ was defined as a subversion zone, i.e. as the lower counterpart of the inversion zone, where shortening of lower crust was accommodated (BABEL Working Group, 1993). Another interpretation previously suggested is that the crustal keel in the Baltic Sea represents underplating by magma that solidified at the base of the crust during the late Carboniferous to earliest Permian magmatic event (Thybo, 2000). Nevertheless, some seismic experiments did not provide evidence for a crustal keel underneath the STZ (DEKORP-BASIN'96 PQ2 profiles; Bleibinhaus et al., 1999; Krawczyk et al., 2002) or TTZ (BalTec WARR profile; Janik et al., 2022) even if its presence was suggested by potential field data in the latter case. This was our motivation for undertaking potential field modelling together with the reinterpretation of the

DEKORP-BASIN'96 PQ2 deep reflection seismic profiles and interpretation of the regional seismic profile from the BalTec project (line BGR16-212).

An extensive sandy shelf extended across much of present-day SW Scandinavia in the Ediacaran with sandstone beds overlying Precambrian crystalline basement (Erlström et al., 1997). These are covered by a thin succession (<100 m) of middle Cambrian to Early Ordovician bituminous alum-shales forming a distinct seismic marker, the O-horizon by Krawczyk et al. (2002). The N-vergent Caledonian deformation complex, comprising Ordovician sediments, is thrust over the EEC basement and its lower Paleozoic sedimentary cover in the SW Baltic Sea (e.g., Berthelsen, 1992; Katzung et al., 1993; Dallmeyer et al., 1999). The complex bends towards the SE farther east, where it approaches the TTZ and subcrops onshore northern Poland (e.g., Figs. 1, 3; Dadlez et al., 1994), where Ordovician and Silurian strata are tightly refolded (e.g., Modliński and Podhalańska, 2010). A northward- and eastward-prograding foreland basin developed in front of the Caledonian orogen during the Late Ordovician-Silurian, onlapping the SW slope of the EEC (e.g., Erlström et al., 1997; Poprawa et al., 1999), and filled with siliciclastic sedimentary succession attaining a maximum thickness of nearly 5000 m (Mazur et al., 2018).

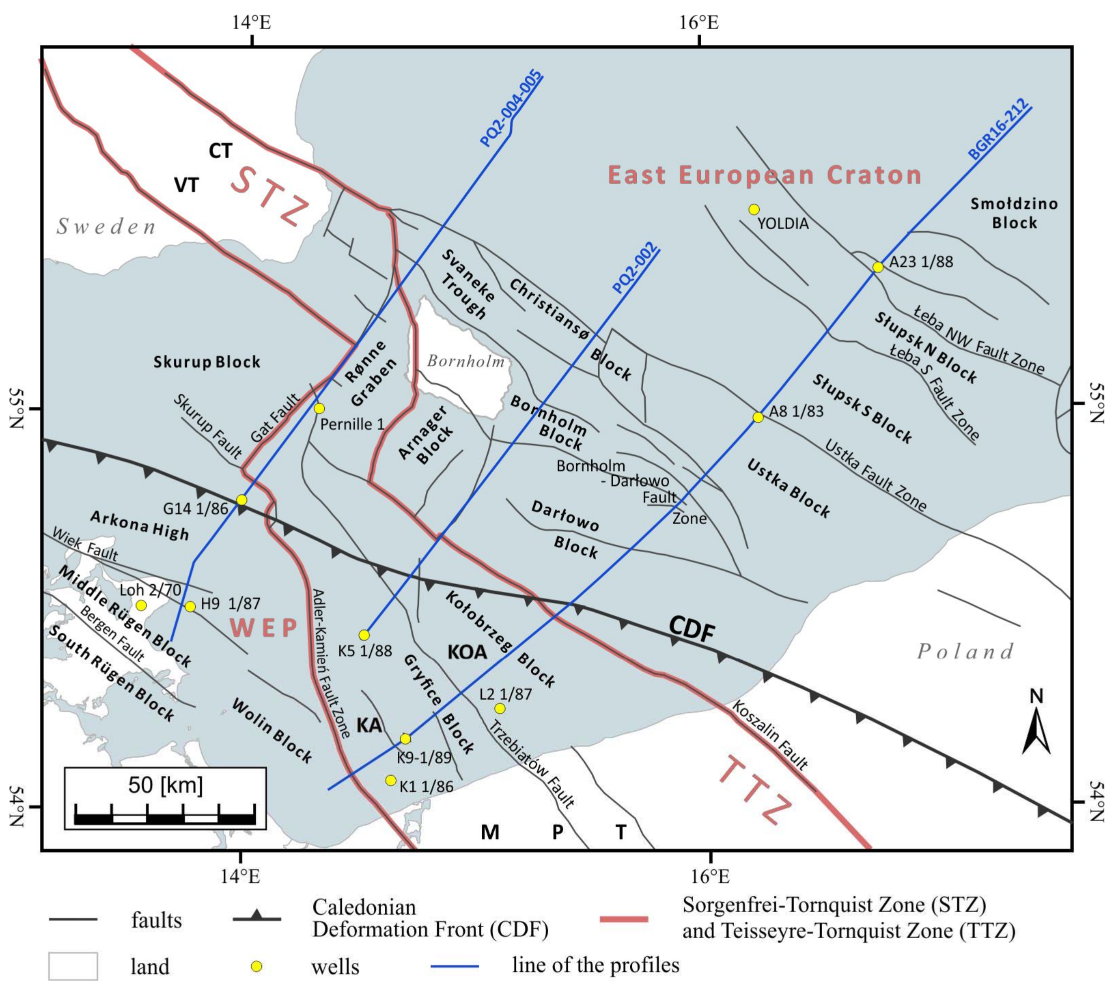

Figure 3. Tectonic map of the southern Baltic Sea. Position of main faults and tectonic blocks are based on Kramarska et al. (1999), Krzywiec et al. (2003), Jaworowski et al. (2010), Pokorski et al. (2010) and Seidel et al. (2018). Location of the STZ and TTZ is modified from Grad et al. (2002). Yellow points refer to the location of offshore boreholes (Erlström et al., 1997; Sopher et al., 2016; Central Geological Database, 2022). Abbreviations: CDF – Caledonian Deformation Front; CT – Colonus Trough; KA – Kamień Anticline; KOA – Kołobrzeg Anticline; MPT – Mid-Polish Trough; STZ – Sorgenfrei-Tornquist Zone; TTZ – Teisseyre-Tornquist Zone; VT – Vomb Trough; WEP – West European Platform.

During Devonian and Carboniferous times, the area of the southern Baltic Sea, as entire NW Europe, was under an extensional regime (Smit et al., 2018). Borehole and reflection seismic data revealed a system of Devonian to upper Carboniferous half grabens in the southern Baltic Sea and its vicinities that developed due to reactivation of Caledonian thrusts (Piske et al., 1994; Lassen et al., 2001; Seidel et al., 2018; Krzywiec et al., 2022). As the entire area was uplifted and eroded during the latest Carboniferous transition from the Variscan orogeny to early Permian rifting (McCann, 1996) the base-Permian discontinuity forms an important seismic regional marker (Vejbæk, 1997). Following the rifting event, the area was onlapped by an extensive Permian-Mesozoic sedimentary basin system with the region of the southern Baltic Sea forming a link between the Danish Basin and the Mid-Polish Trough (e.g., Krawczyk et al., 2002; Krzywiec, 2006a; Maystrenko et al., 2008). The Permian-Mesozoic basin was inverted in the Late Cretaceous to early Paleogene due to a far-field effect of the Alpine convergence (EUGENO-S Working Group, 1988; Erlström et al., 1997; Krzywiec 2002, 2006b; Pan et al., 2022) and North Atlantic ridge push (Mogensen, 1994; Stephenson et al., 2020), the event resulting in widespread uplift and erosion.

The main inversion structures onshore Poland are localized along the NW-SE oriented Mid-Polish Anticlinorium (Fig. 2) that was formed due to inversion of the Mid-Polish Trough, the main depocenter of the Polish Basin (Krzywiec, 2002). The Mid-Polish Anticlinorium continues into the southern Baltic Sea between the Koszalin and Adler-Kamień Fault Zones, where it is split into the Kamień and Kołobrzeg Anticlines (Fig. 2; Krzywiec et al., 2003; Mazur et al., 2005). However, farther north, the inversion axis is shifted NE long the Rønne Graben towards Bornholm and the STZ (Figs. 2, 3). The Rønne Graben was formed in the latest Carboniferous-early Permian as a strike-slip pull-apart basin that subsided during the Mesozoic and underwent inversion with reactivation of faults and development of anticline flexure folds (Liboriussen et al., 1987; Graversen, 2004). Still farther NW, inversion tectonics was focused along the STZ and it was characterized by formation of pop-up structures and pronounced exhumation along the inversion axis concurrent with subsidence at marginal troughs (Pan et al., 2022).

3 Data and Methods

Seismic reflection profiles were combined with gravity and magnetic data to interpret the structure of the crust in the southern Baltic Sea (Fig. 2). We also used public domain borehole data available from previous publications (Erlström et al., 1997; Sopher et al. 2016) and online repository of the Central Geological Database (Central Geological Database 2022) managed by the Polish Geological Institute (http://baza.pgi.gov.pl/).

3.1 Seismic data

Three seismic transects were used in this study to image the structure of the sedimentary strata and deeper crust and provide constraints for potential field modelling (Fig. 2). Two of them come from the offshore part of the DEKORP-BASIN’96 experiment (PQ2 dataset, DEKORP-BASIN Research Group, 1998) including profiles PQ2-004-005 and PQ2-002 located NW and SE of the Bornholm Island, respectively (Fig. 2). The third transect (BGR16-212) is situated nearly parallel to the west Polish coast, halfway between Poland and Bornholm (Fig. 2). This profile was acquired within BalTec project (cruise MSM52) onboard R/V Maria S. Merian (Hübscher et al., 2017). The PQ2 profiles imaged the entire crust down to the Moho and uppermost mantle, whereas profile BGR16-212 provided imaging of sedimentary strata and crystalline basement in the east. Detailed acquisition parameters of both seismic surveys can be found in Krawczyk et al. (2002) and Hübscher et al. (2017), respectively. Most important parameters are summarized in Table 2.

Data were processed up to post-stack time migration (PQ2 profiles) or pre-stack time migration (BalTec). In both cases, the depth conversion was based on the smooth interval velocity field derived from stacking velocities. More details about the processing can be found in Krawczyk et al. (2002) and Nguyen et al. (2023).

Table 2. Acquisition parameters of the DEKORP-BASIN’96 PQ2 and BalTec reflection seismic profiles.

Parameter / Survey	DEKORP-BASIN’96 PQ2	BalTec (cruise MSM52)
Date acquired	1996	2016
Group interval	25 m	12.5 m
Avg. shot interval	75 m	25 m
Min. offset	73,5 m	37,5 m
Max. offset	1500* (2100**)	2700 m
Number of channels	60* (84**)	216
Nominal fold	10* (14**)	54
Airgun array volume	52 l	19.7 l
Record length	26 s	5 s

*PQ2-002 & PQ2-004, **PQ2-005

3.2 Potential field data

The regional gravity data for the southern Baltic Sea come from the Getech's Multi-Sat satellite altimetry-derived gravity product (Green et al., 2019). The original data were gridded at a 0.02° resolution corresponding to c. 2.2 km in the *y* dimension and c. 1.3 km in the *x* dimension. The gravity anomaly map (Fig. 4a) is a compilation of free air gravity offshore and Bouguer gravity onshore. A complete Bouguer correction was calculated using a rock density of 2.67 g/cm^3.

The magnetic data offshore are the marine data (Total Magnetic Intensity) from the Getech's Baltic Sea compilation (Fletcher et al., 2011). The data were gridded at a 0.01° (~1 km) resolution at a common elevation of 1 km above sea level. The reduction-to-pole (RTP) transform was applied to the magnetic anomaly data (Fig. 4b). The RTP transform attempts to simplify the magnetic field by rotating the magnetic vector to be vertical, thereby centering magnetic anomalies above their causative bodies (MacLeod et al., 1993).

3.3 2-D/2.5-D gravity and magnetic modelling

The gravitational and magnetic responses of three 2-D/2.5-D density and susceptibility models along seismic profiles PQ2-004-005, PQ2-002 and BGR16-212 were calculated using XField modelling package (ARK CLS Ltd., 2022) with model layers of infinite length. These models are built from SEG-Y files of the seismic data and modelled against the gridded potential field data sampled along the line of section. XField operates as a plug-in for OpendTect or Petrel, enabling the interpreter to convert seismic horizons into geological bodies within the model. Each model body appears as a polygon to which an average density, interval velocity and magnetic susceptibility can be assigned. The software forward-calculates the gravity and magnetic response of the resulting density and susceptibility models, using the technique outlined in Talwani and Ewing (1960). This allows the user to make modifications to interpreted seismic horizons, density and susceptibility characteristics of the crust, until the forward calculated response of the model satisfies all of the available datasets. The densities used for sedimentary horizons in the course of modelling were obtained from boreholes situated along the profiles or in their proximity. Densities in the crystalline crust were calculated from seismic velocities using the Nafe-Drake formula (Ludwig et al., 1970; Brocher, 2005). The starting susceptibility values for the magnetic basement were adopted from previous modelling studies (Petecki, 2002; Mazur et al., 2016b; Janik et al., 2022).

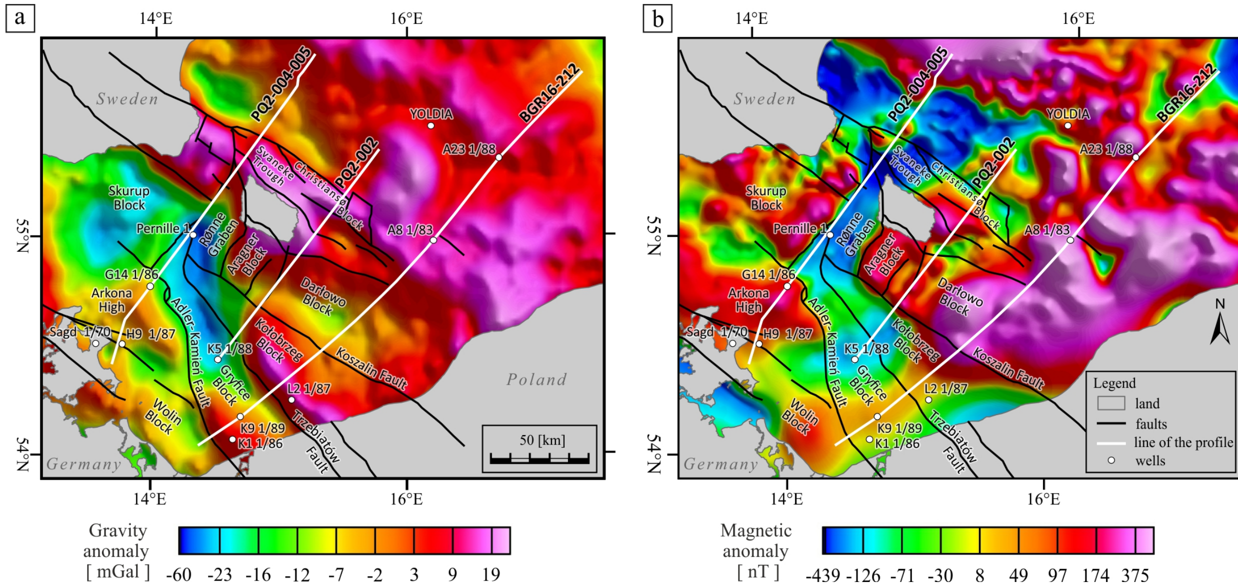

Figure 4. Gravity and magnetic anomaly maps. Location of main faults and tectonic blocks (modified from Seidel et al., 2018) overlaid on the Free Air gravity (a) and Reduced-to-Pole magnetic (b) anomaly maps. Position of the BGR16-212, PQ2-004-005, PQ2-002 profiles and boreholes is indicated. Gravity and magnetic data provided by Getech Group plc.

Gravity and magnetic models are non-unique, i.e., there are a multitude of density and susceptibility configurations that can produce the same amplitude and wavelength anomaly. In addition, attempting to model gridded potential field data in 2-D suffers from the fact that gridded data could be affected by features that are out of the plane of section. Such 3-D effects may have some impact on models, making fitting the observed gravity and magnetic data in some places difficult. Despite these limitations, 2-D/2.5-D models are useful in quantitatively modelling features visible on the seismic data to test models and aid with interpretation in areas where seismic imaging is incomplete. The non-uniqueness issue can also be combated in several ways to increase confidence in the modelling results. First of all, boreholes provide calibration of the shallow parts of the models. Furthermore, the use of geological knowledge and literature research is necessary to produce a reasonable set of modelling parameters. Finally, it is essential to focus interpretation edits on the correct parts of the model, to minimize the residual miss-fit between the model and observed data. By systematically building in all of the elements of the model, using those that we are most confident about first (e.g., seismic horizons), the variables are reduced and the interpretation can be focused on the appropriate section of the crust.

4 Results and Interpretation

We first present seismic interpretation of three seismic reflection transects crossing the southern Baltic Sea in the NE-SW direction (Fig. 2). Then, we show 2-D gravity and magnetic forward models that were built upon the interpreted seismic lines. The paper contains our preferred models, whereas alternative models are included in Supplementary Materials.

4.1 Seismic interpretation of profile PQ2-004-005

Seismic interpretation of profile PQ2-004-005 is well constrained in its upper part due to good seismic imaging of the top basement, presence of four wells penetrating through the majority of sedimentary cover and surface exposures of basement rocks (Fig. 5). Top basement corresponds to a group of high-amplitude reflectors almost along the full length of the profile. Moreover, the identification of the top of basement is confirmed by borehole G-14 that penetrated into the crystalline rocks as well as the exposure of basement at km 120-125 of the seismic section, directly NW of the Bornholm Island (Fig. 2). Seismic imagining within the upper crystalline crust is partly obscured by multiples, but some intra-crustal reflectors are clearly visible as packages of high-energy reflectors (Fig. 5). The intra-crustal reflectors may represent volcanic sills or low-angle extensional shear zones. Similar interpretation was applied to the deep intra-crustal reflector imaged by PolandSPAN line PL1-5400 onshore Poland (Mężyk et al., 2019).

Precambrian crystalline basement jointly with its Phanerozoic sedimentary cover are cross-cut and displaced by several sub-vertical faults. These faults can be subdivided into two groups. One includes faults, whose upward continuation is limited at the base of Triassic. They probably represent a family of Carboniferous extensional faults as documented by a growth fault in the south-westernmost section of the profile at km 5-10. This fault is additionally constrained by borehole Sagd 1/70 (Fig. 5a). Activity of some of these faults must have been renewed in the early Permian as demonstrated by localized increase of the Permian thickness above the tectonic graben at km 75-85 of the profile (Fig. 5a). The second group of faults comprise features that cut through the entire sedimentary pile up to the base of Cenozoic. Their connection with the Late Cretaceous (Alpine) inversion of the Permian-Mesozoic basin (Mazur et al., 2005; Kley, 2018; Stephenson et al., 2020; Krzywiec et al., 2022) seems likely. They are reverse faults with either NE (km 50-100) or SW wall (km 125-150) elevated. Between km 125-150 of the profile reverse faults create c. 1 km deep syn-inversion marginal troughs filled with Cretaceous sediments and capped by thin Cenozoic strata (Fig. 5a). This provides evidence for the duration of the Alpine basin inversion and syn-inversion sedimentation practically to the end of the Cretaceous. Furthermore, there is no evidence that the reverse faults represent older features that were inverted in the Late Cretaceous. Therefore, it seems that the second group of faults recognized along the profile includes thick-skinned features created in response to Late Cretaceous compression.

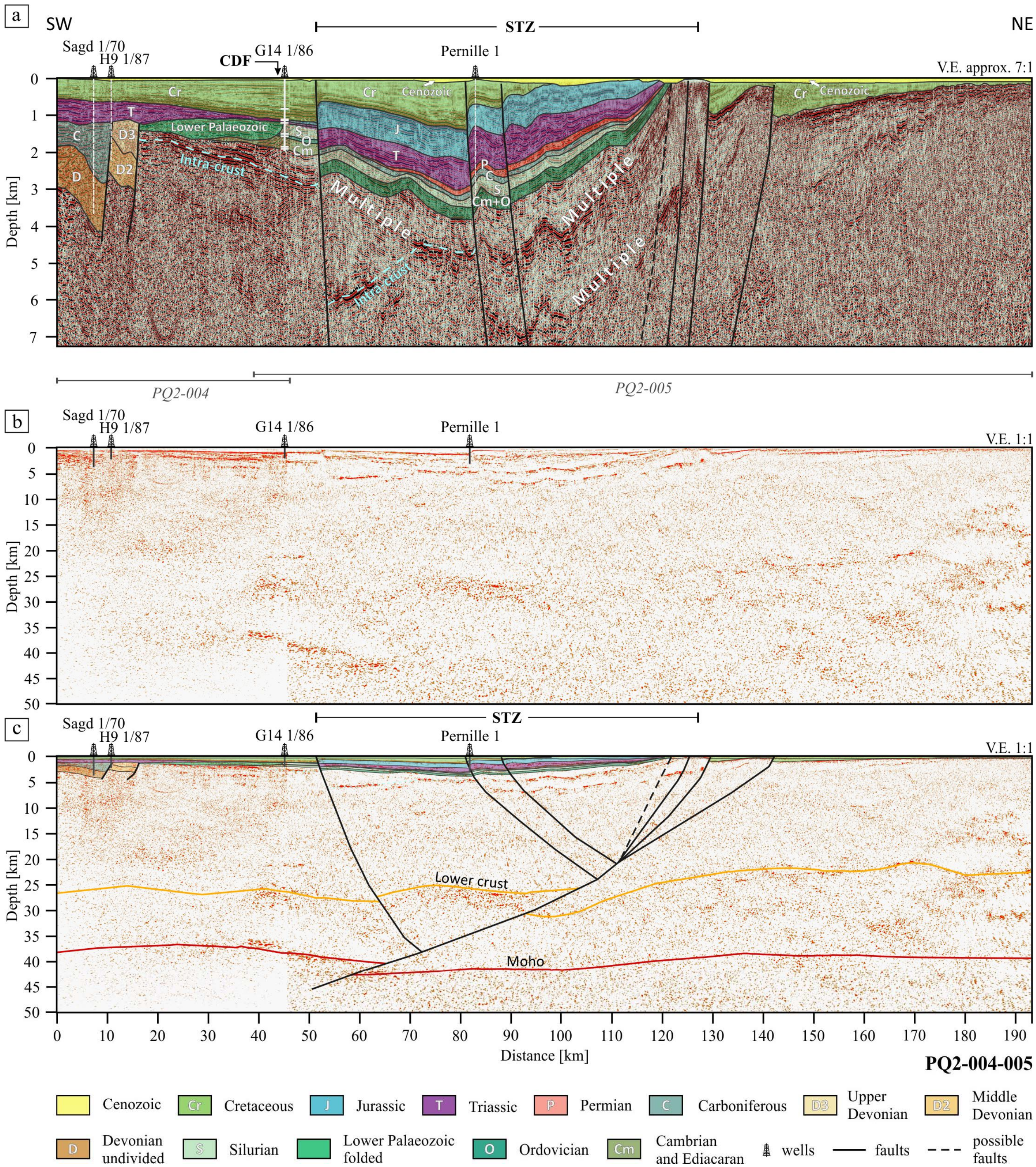

Figure 5. Seismic interpretation of the PQ2-004-005 profile. Vertical exaggerations are 7:1 for the upper part of the profile, and 1:1 for the full profile. CDF – Caledonian Deformation Front, STZ – Sorgenfrei-Tornquist Zone. Uninterpreted upper 7 km are shown in Figure SM1. Trace envelope attribute is displayed in panels (b) and (c).

The CDF is not well imaged by profile PQ2-004-005. This feature is located directly SW of the G-14 borehole, i.e., somewhat farther to the NE than previously postulated (Berthelsen, 1992). The total thickness of deformed lower Paleozoic (Ordovician?) sediments is below 1 km that emphasizes a thin-skinned character of deformation. Furthermore, the layer of the lower Paleozoic is discontinuous toward the SW, being cut by a late Paleozoic fault at km 20 of the profile. However, lower Paleozoic cannot be recognized on seismic section in the footwall of the fault (Fig. 5a). Possibly, the fault was developed as a reverse one and, thus, the lower Paleozoic was eroded in the present-day footwall. Consequently, seismic interpretation suggests a polyphase activity of the fault located NE of the H9 1/87 borehole – first as a reverse feature before Devonian, then extensional normal fault in the Middle-Late Devonian and Carboniferous, and, finally, again as a reversed fault at the end of Carboniferous.

The lower crust imaged by profile PQ2-004-005 is characterized by clusters of rather short, high-amplitude reflectors (Fig. 5b). Their rapid disappearance upward the section defines the top of the lower crust and the transition to the mostly transparent middle crust. This interface was earlier interpreted as the Moho discontinuity (e.g., Krawczyk et al., 2002). The Moho identified in this study is deeper and only partially imaged, being in places recognizable as a top of clusters consisting of dense high-amplitude reflections (Fig. 5b, c). Both the Moho and lower crust are displaced by a crustal-scale thick-skinned NE-vergent thrust (Fig. 5b, c) extending upward to the base of Cenozoic (Fig. 5a, c). The near-surface expression of the thrust corresponds to three reverse faults at km 125-140 of the profile. Furthermore, the lower crust is also displaced by a back-thrust that is linked to a reverse fault at 50 km of the profile. The combination of a thrust and back-thrust explains the shift in a position of hanging-walls of the Cretaceous faults, changing from the SW to NE (Fig. 5).

4.2 Seismic interpretation of profile PQ2-002

Seismic interpretation of profile PQ2-002 is constrained by only one deep borehole K5 1/88. Nevertheless, the well is situated in the south-westernmost part of the profile, where the sedimentary cover is thickest (Fig. 6a). Farther NE, a pile of sediments is much thinner with a basement exposure at c. km 75 of the profile, the configuration making interpretation less complicated. The top basement is expressed by a group of high amplitude reflectors along the most of the profile. The reflectivity of the upper crystalline crust is changeable from stronger in the NE section of the profile to weaker in the SW section. The reflections pattern in the NE part of the line is additionally complicated by multiples. The geometry of the top of basement is characterized by a relatively steep slope between km 0 and 30 (Fig. 6a). The lowering of the top basement created an accommodation space for a c. 5 km thick sedimentary pile. Its lower part corresponds to the deformed lower Paleozoic sediments (Caledonides) confirmed by borehole K5 1/88. The seismic image shows a thin-skinned character of deformation and the weakly marked CDF. The lower Paleozoic sediments are capped by a relatively thin layer of Carboniferous sandstones (Erlström et al., 1997) that is missing farther NE. The increased subsidence characterized the SW part of the profile also in the Permian-Mesozoic. The SW-ward thickening of Permian, Triassic and Jurassic strata demonstrates a prolonged basin deepening within the offshore continuation of the Mid-Polish Trough. Only the Cretaceous thickness pattern is unrelated to the basement slope along the first 30 km of the profile.

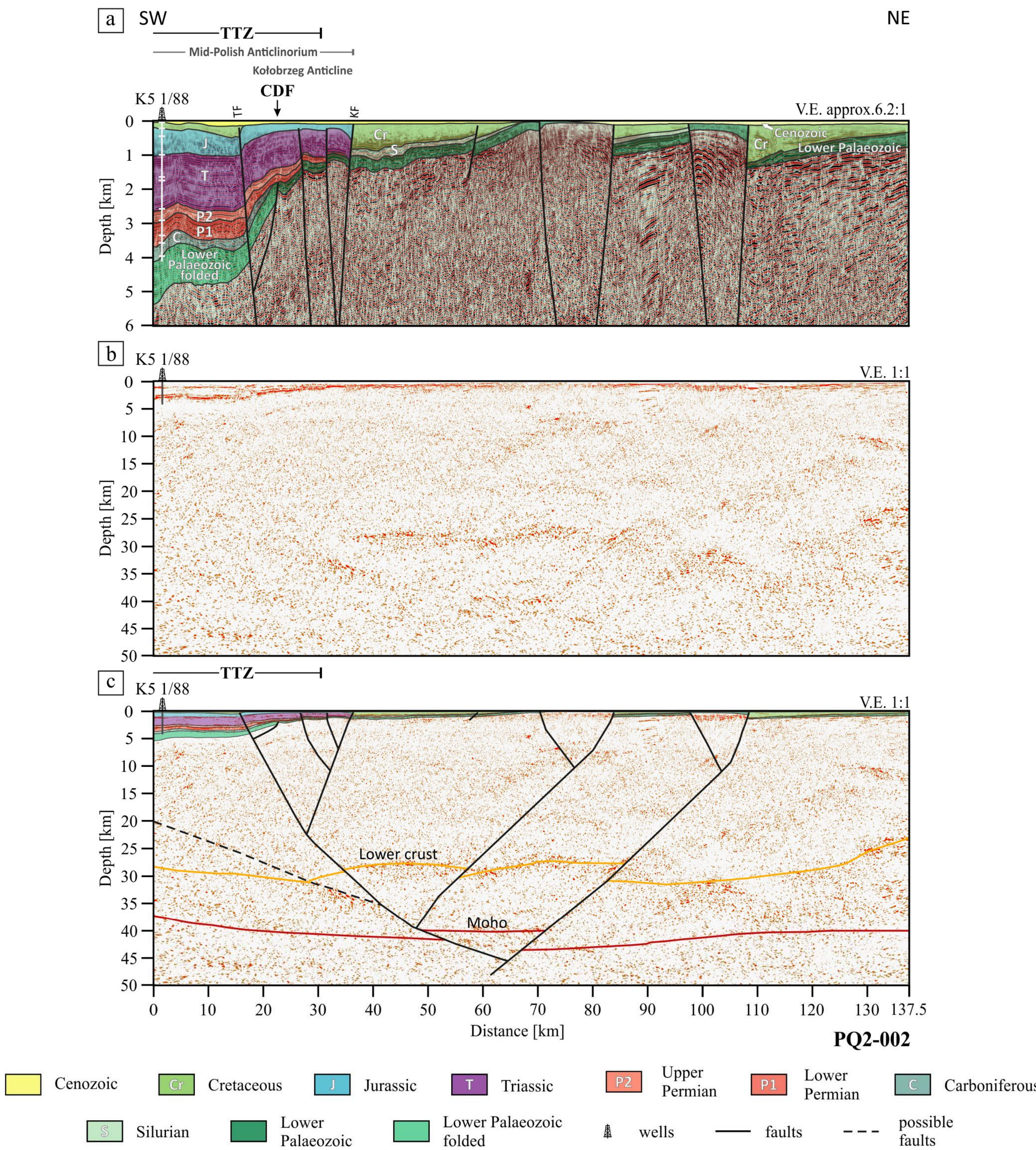

Figure 6. Seismic interpretation of the PQ2-002 profile. Vertical exaggerations are 6.2:1 for the upper part of the profile, and 1:1 for the full profile. CDF – Caledonian Deformation Front, TTZ – Teisseyre-Tornquist Zone. Uninterpreted upper 6 km are shown in Figure SM1. Trace envelope attribute is displayed in panels (b) and (c).

The upper part of the crystalline crust and its sedimentary cover is cut and displaced by several reversed faults with their vergence changing from SW to NE (Fig. 6a). Most of them terminates at the base of Cenozoic separating the basement into several elevations and depressions. The increased Cretaceous thickness on footwalls confirms the syn-sedimentary character of faulting, most likely related to the Late Cretaceous, Alpine inversion of the German-Polish Basin (Kley, 2018; Krzywiec et al., 2022). The fairly uniform thickness of pre-Cretaceous strata cut by the faults indicates that they formed as new features due to Late Cretaceous inversion. At km 10 to 30, there occurs another inversion-related structure, the Kołobrzeg Anticline with Jurassic sediments at the base Cenozoic surface (Fig. 6a).

At the crustal scale, profile PQ2-002 shows thick-skinned thrust tectonics related to Late Cretaceous shortening. Thrust planes cut through the entire crust displacing the Moho and top of the lower crust (Fig. 6b, c). The NE-vergent thrusts are associated with a backthrust having an opposite polarity, the structural pattern well explaining the changeable polarity of the reversed faults imaged at the shallow level (Fig. 6a). The lower crust is characterized by the increased reflectivity compared to the middle and upper crust. The top of the lower crust corresponds to clusters of discontinuous high-energy reflections (Fig. 6b, c). The Moho is only revealed in places by groups of higher-amplitude reflectors standing out against the background of transparent crust or upper mantle. Similarly, Moho is interpreted as being much deeper than postulated by Krawczyk et al. (2002).

4.3 Seismic interpretation of profile BGR16-212

Imaging along profile BGR16-212 was only possible down to ~10 km depth due to the acquisition parameters applied (Fig. 7). However, we supplement interpretation of the deeper crust and the Moho from the results of the coinciding WARR profile (Janik et al., 2022). The top basement is expressed by a few high amplitude reflectors along the most of the profile (up to the TTZ). Its position is confirmed by two boreholes, A8 1/83 and A23 1/88 (Fig. 7), that reached crystalline basement rocks in the central and NE part of the seismic line. Three other boreholes, K1 1/86, K9 1/89 and L2 1/87, penetrated a sedimentary succession in the SW section of the profile. Two of them were terminated in Devonian rocks and one (L2 1/87) reached highly deformed Ordovician sediments (Fig. 7).

The profile from km 80 to its NE termination is characterized by the relatively flat top of basement plunging to the SW at a low angle. Consequently, the thickness of overlying sediments increases SW-ward from 1 to 4 km (Fig. 7). Farther SW, between km 40 and 80, the profile shows a steep slope of the top basement rapidly increasing its depth down to 10 km. Furthermore, along the first 40 km of the profile, the basement is not imaged because it lies below a depth of 10 km. The upper crystalline crust is mostly transparent along the profile with just sparse multiples. Only a group of reflectors near the NE end of the line at a depth of 2.5 km may correspond to real features probably representing magmatic sills.

The sedimentary cover in the NE half of the profile consists of lower Paleozoic sediments that are only slightly disturbed by sub-vertical faults that are rooted in the basement and terminate at the base Cenozoic (Fig. 7). Thick Silurian strata represent largely undeformed sediments of the Caledonian foreland basin. A thicker Cretaceous succession (up to 1 km) exists between km 75 and 125 of the profile comprising sediments of a syn-inversion marginal trough.

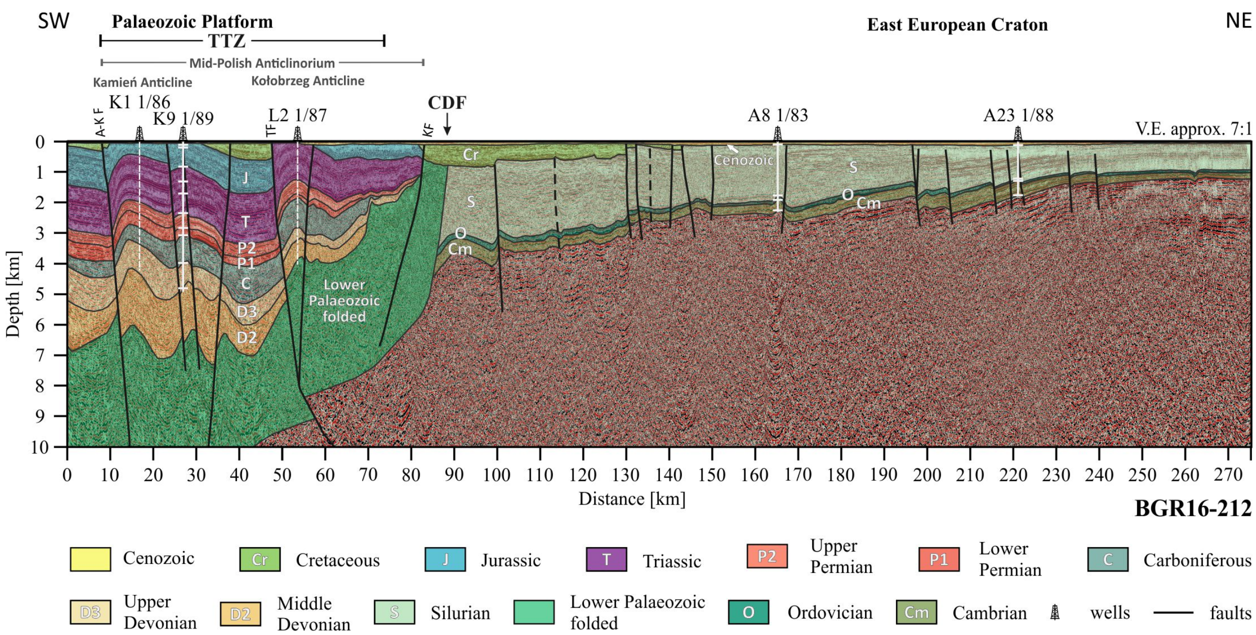

Figure 7. Seismic interpretation of the BGR16-212 profile. Vertical exaggeration is 7:1. CDF – Caledonian Deformation Front, TTZ – Teisseyre-Tornquist Zone. Uninterpreted data are shown in Figure SM1.

The thick sedimentary pile along the first 80 km of the profile consists in 40-50% of the strongly deformed lower Paleozoic (Ordovician?) sediments of the North German-Polish Caledonides. The presence of such rocks is verified by borehole L2 1/87 (Fig. 7). The lower Paleozoic succession terminates toward the NE against the crystalline basement slope with the CDF splitting upward from the sediments directly overlying the top of the basement near the upper tip of the slope. This geometry suggests a thin-skinned character of Caledonian deformation with a detachment horizon possibly located within the alum-shales. The correlation between the position of the CDF and basement slope suggests a buttressing effect of the latter on the NE-ward propagation of the Caledonian orogenic wedge.

The lower Paleozoic succession SW of the CDF is overlain by thick Devonian and Carboniferous sediments attaining a thickness of c. 2 and 1 km, respectively (Fig. 7). This suggests that the area SW of the CDF was subject to further subsidence and basement lowering after the emplacement of the Caledonian orogenic wedge. The Carboniferous strata are truncated at the top by the base Permian (Variscan) unconformity indicating uplift and erosion. Deposition of c. 4 km thick Permian-Jurassic strata overlying the unconformity indicates substantial subsidence during Permian-Mesozoic times in the part of the Mid-Polish Trough intersected by the SW part of the profile. Cretaceous sediments are thin and discontinuous, but this is probably an effect of uplift and erosion during and after the Late Cretaceous-Paleocene basin inversion.

The SW section of profile BGR16-212 reveals strong inversion of the Permian-Mesozoic depocenter representing the NW part of the Mid-Polish Trough. Inversion tectonics created two regional-scale folds in this area, the Kamień and Kołobrzeg anticlines, at the top of which Jurassic and Triassic sediments are exposed at the sea bottom, respectively. (Fig. 7; Mazur et al., 2005). The anticlines are accompanied by a few subvertical reverse faults (Fig. 7).

4.4 2-D gravity and magnetic model for profile PQ2-004-005

The boundaries of model bodies are defined by seismic horizons and faults interpreted in seismic profile (Fig. 5). The densities and susceptibilities used in the model are summarized in Table 3 and, for the crystalline crust, showed in Figure 8d. In the course of modelling, we tried to maintain a relatively narrow range of density variation for specific lithologies to avoid unnecessary complexity of the solution applied. The synthetic response of the model produces a good match compared to the observed gravity profile with RMS error of 8.27 mGal (Fig. 8a). The observed gravity profile is smooth as we used free-air gravity anomaly data derived from satellite altimetry. This data set is devoid of a short-wavelength frequency band owing to the sensitivity of the acquisition method. Gridding at a 0.02° resolution additionally contributed to smoothing the data. The synthetic response of the model produced a number of short-wavelength anomalies related to the seismically-controlled geometry of the top of basement (Fig. 8). Thick-skinned reverse faults and pop-up structures constitute shallow sources of short-wavelength density contrasts between basement and sedimentary cover. Anomalies generated by these contrasts are missing from the satellite gravity data being the reason for majority of misfit observed in the model.

The long-wavelength gravity anomalies are mostly controlled by configuration of the top of the basement (Fig. 8). This relationship is the best exemplified by the basement low in the vicinity of the Pernille 1 borehole (km 40-110) and the basement high NE of it (km 110-150). A broad gravity low is observed over the basement depression between km 40 and 110 of the profile, corresponding to two-thirds of the STZ width (Fig. 8). This anomaly is comparable to gravity lows associated with the TTZ farther south onshore and offshore Poland (Mazur et al., 2016b; Janik et al., 2022). However, in contrast to the TTZ, the basement depression imaged by profile PQ2-004-005 entirely accounts for the long-wavelength negative anomaly associated with the STZ since it is filled with low-density sediments (Fig. 8). The relationship between the gravity anomalies and the top basement geometry is less recognizable along the SW section of the profile (km 0-40). This is because of the lesser density contrast between the basement and the lower Paleozoic and Devonian-Carboniferous sediments. As the base Mesozoic (Variscan) unconformity is nearly horizontal in this area, the observed and modelled gravity profiles are flat as well (Fig. 8). The large late Paleozoic half-grabens identified by seismic data near the SW end of the profile are not recognized in potential field data. The CDF is also practically undetectable by gravity and magnetic data which confirms its thin-skinned character. Finally, the Moho and top of the lower crust seems to have a limited impact on the gravity response since both horizons are generally flat (Fig. 8).

Table 3. Key for density and susceptibility values used in the modelling of profiles PQ2-002, PQ2-004-005 and BGR16-212.

Colour	Blocks	Density [g/cm^3]	Susceptibility [SI]
	Baltic Sea	1,03	
	Quaternary	2,03	
	Cretaceous	1,92 - 2,3	
	Jurassic	2,1 - 2,40	
	Triassic	2,3 - 2,52	
	Upper Permian	2,46 - 2,67	
	Lower Permian	2,36 - 2,44	
	Permian undivided	2,55	
	Carboniferous	2,56 - 2,60	
	Upper Devonian	2,62 - 2,67	
	Middle Devonian	2,66 - 2,67	
	Devonian undivided	2,66	
	Silurian	2,55 - 2,62	
	Ordovician unfolded	2,62 - 2,68	
	Lower Palaeozoic folded	2,66 - 2,68	
	Cambrian	2,44 - 2,66	
	Cambrian-Ordovician undivided	2,65	
	Upper mantle	3,3	
BGR16-212			
	Upper crust	2,82	0,077
	Middle crust	2,92-2,95	0,04-0,06
	Lower crust	2,97	
PQ 002			
	Upper/Middle crust	2,76 - 2,81	0,035 - 0,065
	Lower crust	2,9 - 2,95	0,02 - 0,04
PQ 004-005			
	Upper/Middle crust	2,79 - 2,82	0,025 - 0,04
	Lower crust	2,9 - 2,95	0,01 - 0,025

The synthetic magnetic data produce a very large RMS error of 422.74 nT. Nevertheless, the observed and synthetic magnetic profiles are not totally inconsistent (Fig. 8b). Their shapes along the majority of the profile are comparable suggesting that the geometry of the top of basement was accurately recognized by seismic data. However, attaining a better fit to the observed magnetic anomalies would require splitting the magnetic basement into several blocks with subvertical boundaries and varying susceptibility. Such model bodies would correctly represent lateral susceptibility variation of the basement rocks but their geological significance would remain unclear. Therefore, to avoid excessive complexity of the geological model, we accepted a large RMS error of the modelled magnetic profile.

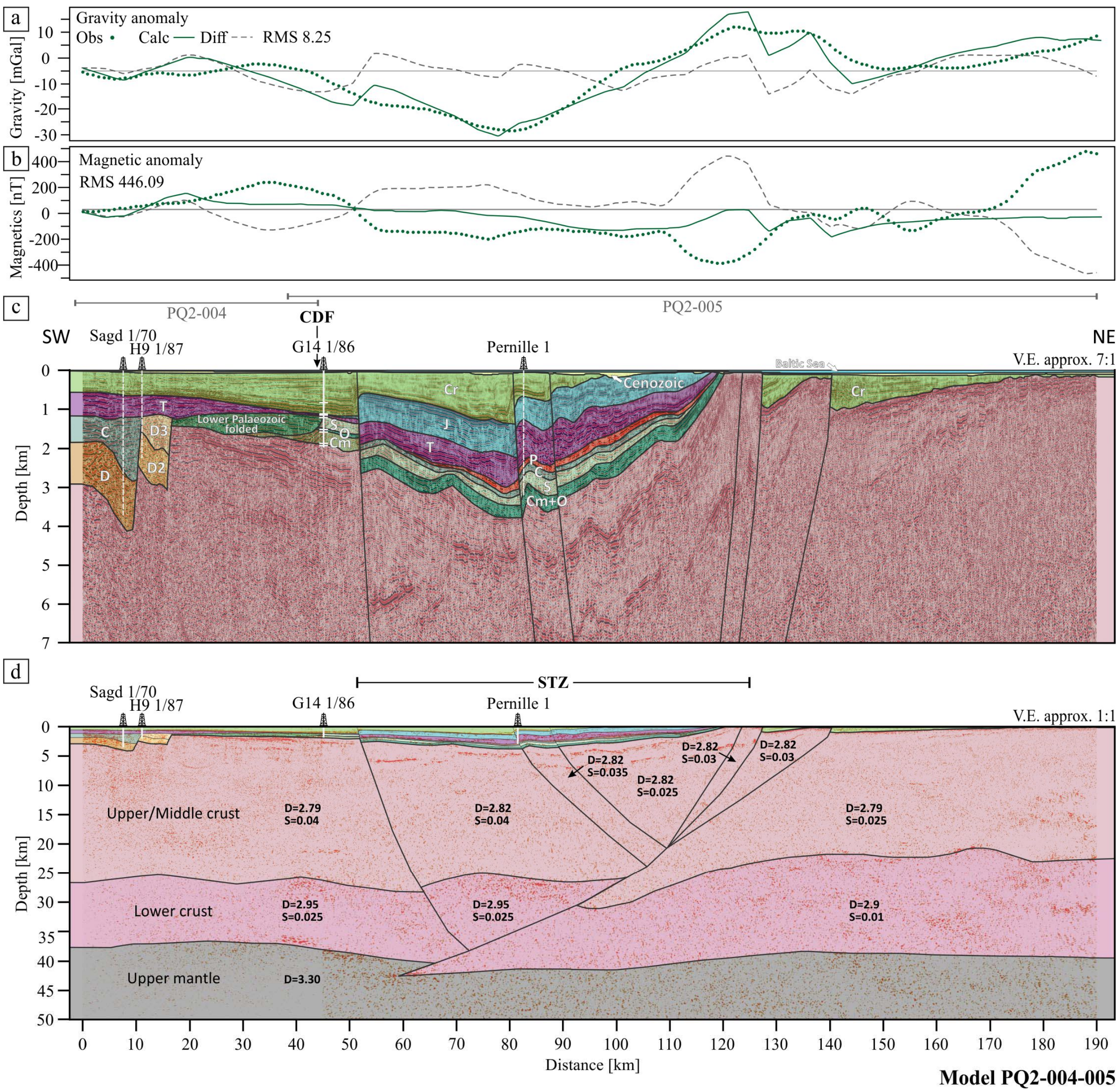

Figure 8. Two-dimensional gravity and magnetic model for the PQ2-004-005 profile. (a, b) – gravity and magnetic data, respectively. Green, dotted lines – observed and green, solid lines – modelled. Grey, dashed line shows the magnitude of error. (c) – vertically exaggerated (7:1) upper part of the geological model. (d) – vertically exaggerated (1:1) full geological model based

on the seismic profile. Numbers indicate densities (D) in g/cm^3 and susceptibilities (S) in SI convention. Abbreviations: CDF – Caledonian Deformation Front; STZ – Sorgenfrei-Tornquist Zone.

Since the current interpretation of the Moho depth is different from previous interpretations based on the same seismic data (Bleibinhaus et al., 1999; Meissner and Krawczyk, 1999; Krawczyk et al., 2002), we performed additional tests which are included in Supplementary Materials (Fig. SM2). We created an alternative gravity and magnetic model using the Moho horizon from Bleibinhaus et al. (1999) to calculate the synthetic gravity and magnetic response. In addition, the same approach was repeated using the Moho horizon extracted from the Moho map by Maystrenko and Scheck-Wenderoth (2013), the latter derived from seismically constrained 3-D inversion of gravity data. Both alternative solutions show much higher RMS errors compared to the model built upon the current interpretation of the Moho depth (Fig. SM2). Nevertheless, the Moho horizon by Maystrenko and Scheck-Wenderoth (2013) is noticeably closer to the current interpretation fully matching it NE of the STZ (Fig. SM2). The misfit of the magnetic profiles for both alternative models are also high like in the preferred interpretation (Figs. 8, SM2).

4.5 2-D gravity and magnetic model for profile PQ2-002

As for the previous model, seismic horizons and faults were used to define boundaries of the model bodies (Fig. 6). For the densities and susceptibilities applied see Table 3 and, for the crystalline crust, also Figure 9d. We used the similar approach as in the previous model, trying to keep a range of density and susceptibility variation for specific lithologies as narrow as possible. The synthetic response of the model produces a good match to the observed gravity profile with RMS error of 7.72 mGal (Fig. 9a). Again, as we used free-air gravity anomaly data derived from satellite altimetry the gravity profile along line PQ2-002 is smooth. Therefore, several short-wavelength anomalies of the synthetic profile produced by the geometry of the top basement do not match the observed data (Fig. 9). Seismically-constrained thick-skinned reverse faults and pop-up structures generate short-wavelength gravity anomalies that are missing from the satellite gravity data causing the misfit between the synthetic and observed gravity profiles (Fig. 9).

As in the previous model for line PQ2-004-005, the long-wavelength gravity anomalies are controlled by configuration of the top of basement (Fig. 9). Two basement horsts at c. km 75 and 105 generate two regional gravity highs. By contrast, the basement low along the first 30 km of the profile is the source of a negative gravity anomaly. However, in contrast to the more southerly sections of the TTZ (Mazur et al., 2016b; Janik et al., 2022), the broad gravity low is entirely related to the low-density sediments within the offshore continuation of the inverted Mid-Polish Trough. Similarly to line PQ2-004-005, the CDF is practically undetectable by gravity and magnetic data (Fig. 9) that confirms its thin-skinned character. Also, the Kołobrzeg Anticline, the major inversion structure, does not produce significant anomalies in the observed data. However, the anticline is well-manifested in the synthetic profile due to low density of the

Cretaceous syn-inversion sediments. Finally, the Moho and top of the lower crust have a limited impact on the gravity profile since both these horizons are generally flat (Fig. 9).

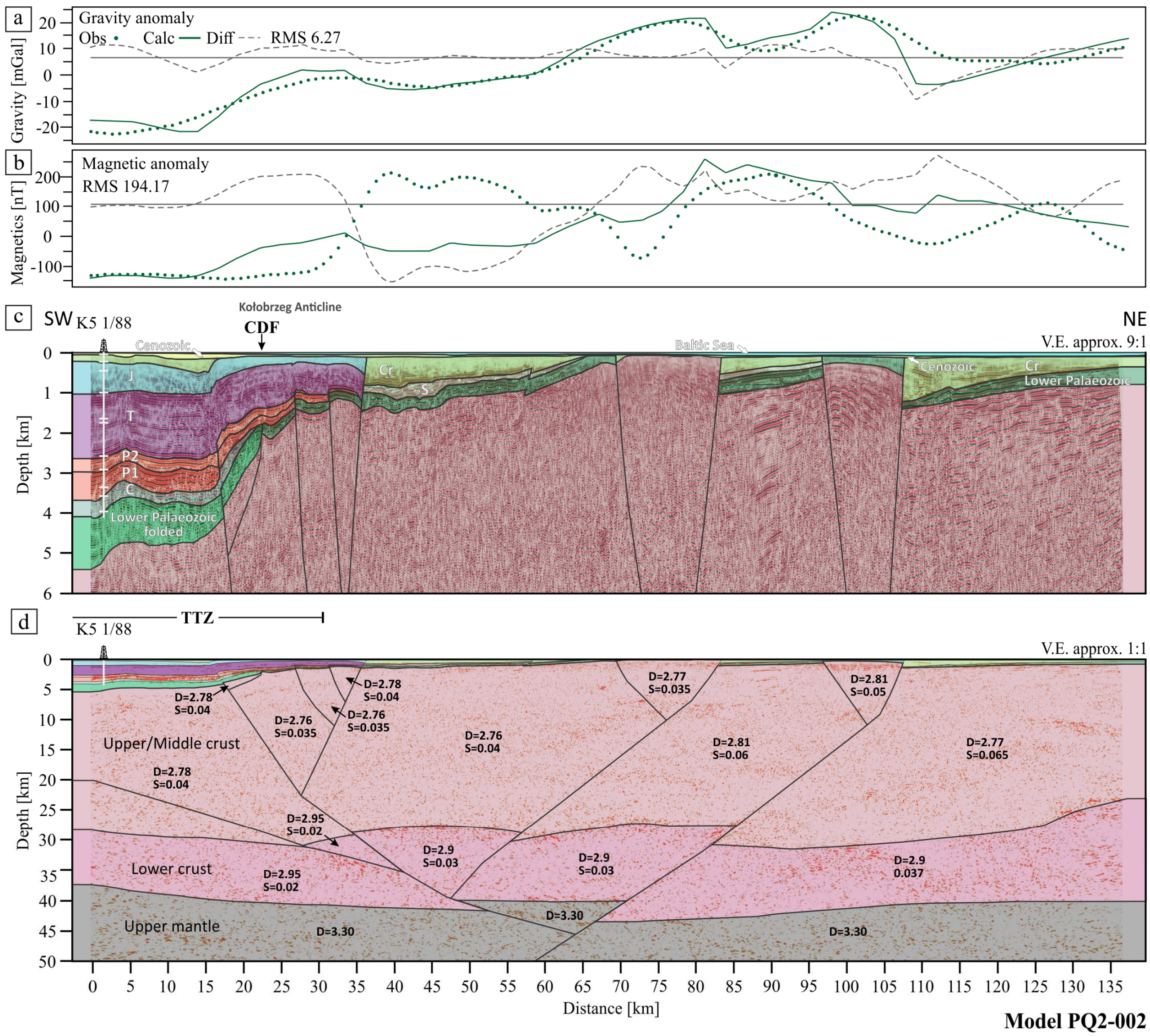

Figure 9. Two-dimensional gravity and magnetic model for the PQ2-002 profile. (a, b) – gravity and magnetic data, respectively. Green, dotted lines – observed and green, solid lines – modelled. Grey, dashed line shows the magnitude of error. (c) – vertically exaggerated (9:1) upper part of the geological model. (d) – vertically exaggerated (1:1) full geological model based on the seismic profile. Numbers indicate densities (D) in g/cm^3 and susceptibilities (S) in SI convention. Abbreviations: CDF – Caledonian Deformation Front; TTZ – Teisseyre-Tornquist Zone.

The synthetic magnetic data produce RMS error of 199.60 nT that is large but smaller than along the profile PQ2-004-005 (Fig. 9b). There are two main sources of misfit: (1) lateral susceptibility variation in the crystalline basement, and (2) resolution of the regional magnetic data set that is devoid of a higher frequency band. The large positive anomaly observed between km 30 and 65 of the profile is absent from the synthetic model response due to the first reason. As already mentioned, we refrained from splitting the magnetic basement into vertical blocks to replicate the lateral susceptibility variation since such an approach would lack geological justification. The short-wavelength anomalies are associated in the synthetic magnetic profile with local uplifts of the crystalline basement but absent from the observed regional data because of the second reason i.e., their limited resolution.

We tested depth to the Moho for profile PQ2-002 using a similar approach as for profile PQ2-004-005. The motivation was the difference in the position of the Moho between the present seismic interpretation and the results of previous studies based on the same seismic data (Bleibinhaus et al., 1999; Meissner and Krawczyk, 1999; Krawczyk et al., 2002). We created alternative gravity and magnetic models using the Moho horizon from the seismic results by Bleibinhaus et al. (1999) and the Moho map by Maystrenko and Scheck-Wenderoth (2013), the latter derived from 3-D inversion of gravity data. Both alternative solutions show significantly higher RMS errors compared to the preferred model using our seismic interpretation (Fig. SM3). The Moho horizon form Maystrenko and Scheck-Wenderoth (2013) is closer to the current interpretation although it gives larger RMS error compared to the Moho by Bleibinhaus et al. (1999). The misfit of the magnetic profiles for all the models is mostly independent from the Moho solution applied (Figs. 9, SM3).

4.6 2-D gravity and magnetic model for profile BGR16-212

Since the seismic reflection data for profile BGR16-212 provide imaging only to a depth of 10 km (Fig. 7) we additionally used the south-westernmost part of the top of basement, top of middle crust, top of lower crust and Moho from the coinciding WARR profile by Janik et al. (2022). For the Moho, we also employed the Moho horizon extracted from the map by Maystrenko and Scheck-Wenderoth (2013) and locally made our own adjustments (Fig. 10). Table 3 as well as Figure 10d provides an overview of densities and susceptibilities applied. The synthetic response of the model produces a good match to the observed gravity profile with RMS error of 8.40 mGal. Similarly to previous models, several short-wavelength anomalies of the synthetic profile produced by the geometry of the top basement do not match the observed data (Fig. 10). However, this problem is less evident for line BGR16-212 because the top of basement imaged along the BGR16-212 profile is smoother than those imaged in the PQ2 lines (Figs. 5, 6).

In contrast to the PQ2 profiles, the long-wavelength gravity anomalies are not to a large extent controlled by the depth to basement. Two major inversion-related anticlines developed within sedimentary strata, the Kamień and Kołobrzeg Anticlines, generate important positive gravity anomalies that are satisfactorily replicated by the model (Fig. 10). Furthermore, the large gravity low between km 70 and 120 of the profile is not centered over the basement depression of the offshore prolongation of the Mid-Polish Trough, but it is located above the elevated basement at the edge of the Precambrian Platform (Fig. 10). Therefore, the cover of low-density sediments cannot compensate for a mass deficit manifested by the anomaly. Referring to experiments in Janik et al. (2022) and earlier views summarized in Mazur et al. (2016b), we implemented a low-density body in the middle crust to compensate for the anomaly in question. Regardless the nature of this body (see discussion in Mazur et al., 2016b and Janik et al., 2022) it allows to achieve a good fit between the observed and modelled gravity profiles. Without a low density body, a big long-wavelength misfit exists in the model and the RMS error is more than tripled (Fig. SM4). The body in the model plays the same role as a crustal keel earlier implemented in 2-D gravity models onshore Poland (Mazur et al., 2015, 2016b). As in the previous models, the location of the CDF is untraceable using potential field data (Fig. 10), the observation that is consistent with its thin-skinned character (Mazur et al., 2016b).

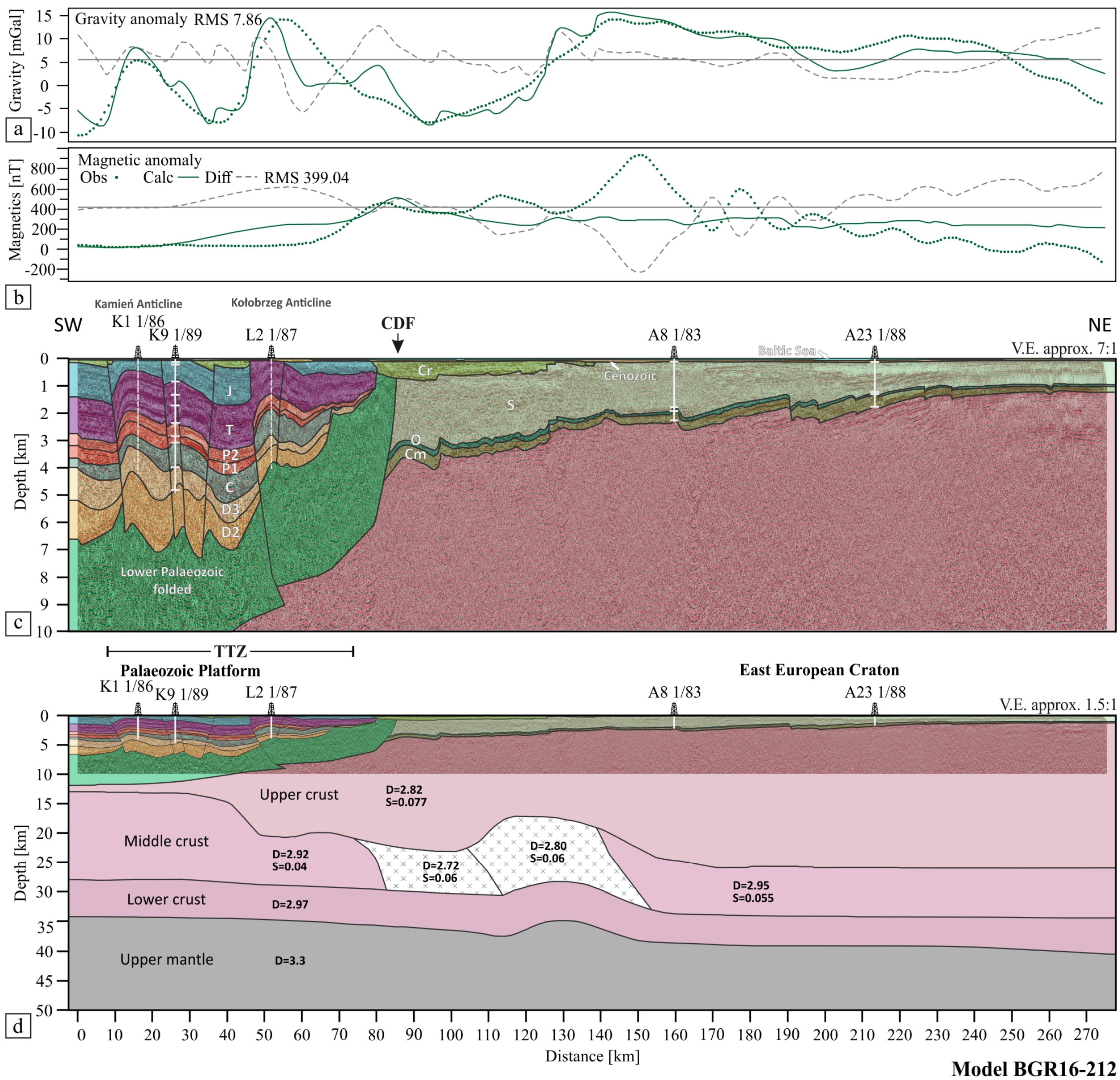

Figure 10. Two-dimensional gravity and magnetic model for the BGR16-212 profile. (a, b) – gravity and magnetic data, respectively. Green, dotted lines – observed and green, solid lines –

modelled. Grey, dashed line shows the magnitude of error. (c) – vertically exaggerated (7:1) upper part of the geological model. (d) – vertically exaggerated (1.5:1) full geological model based on the seismic profile. Thick red line in (d) represents the top of crystalline basement. Numbers indicate densities (D) in g/cm^3 and susceptibilities (S) in SI convention. Abbreviations: CDF – Caledonian Deformation Front; TTZ – Teisseyre-Tornquist Zone.

Although synthetic magnetic data produce large RMS error of 408.42 nT, the observed and synthetic magnetic profiles are not totally incompatible (Fig. 10). Their general outline along the BGR16-212 line is similar, confirming the geometry of the seismically determined top of the basement. Big misfits are related to short-wavelength and high-amplitude magnetic anomalies presumably related to lateral susceptibility variations. Therefore, attaining a better fit to the observed magnetic anomalies would require splitting the magnetic basement into subvertical blocks with various susceptibility. Since the top of basement is relatively smooth along the BGR16-212 line the inconsistency of synthetic and observed magnetic profiles above basement-rooted inversion structures are less apparent compared to the PQ2 seismic lines.

Although no earlier interpretations of the Moho were published for the BGR16-212 profile based on seismic reflection data, we made similar tests as for the PQ2 seismic lines building alternative models (Fig. SM5). This time, we used the Moho horizons from the WARR profile by Janik et al. (2022) and the Moho map by Maystrenko and Scheck-Wenderoth (2013). Both alternative solutions (Fig. SM5) show significantly higher RMS errors compared to our preferred model presented in this paper. It is important to note, that all three Moho horizons by Janik et al. (2022), Maystrenko and Scheck-Wenderoth (2013), and the present study are close each other along the BGR16-212 profile and the significantly higher RMS error for the former two is related to the lack of a low-density body in the middle crust (Fig. SM5). For the same reason, the RMS errors of the magnetic synthetic profiles are almost identical.

5 Discussion

By combining the analysis of regional seismic profiles with the integration of potential field data, we have unveiled several findings that hold relevance on both a local and over-regional scale. These discoveries pertain to various aspects, including the intricate crustal composition beneath the southern Baltic Sea, the character of the boundary demarcating the Precambrian Platform of Eastern Europe and the Paleozoic Platform of Western Europe, and the underlying mechanisms driving basin inversion within a cratonic zone.

5.1 Depth to Moho

The earlier interpretations of the DEKOROP BASIN profiles (PQ profiles) in the southern Baltic Sea postulated shallow Moho at a depth of 28 to 35 km (Krawczyk et al., 2002, their fig. 10). In these interpretations, the Moho is approximately flat at a shallow depth of c. 30 km both SW and NE of the STZ and TTZ (e.g., Bleibinhaus et al., 1999; Meissner and

Krawczyk, 1999; Krawczyk et al., 2002; see also Figs. SM1-2). Nevertheless, the majority of depth-to-Moho studies assumed a strong depth gradient across the STZ and TTZ, implying Moho shallowing by c. 8 km from NE to SW (e.g., Ziegler and Dèzes 2006; Yegorova et al., 2007; Tesauro et al., 2008; Grad et al., 2009; Maystrenko and Scheck-Wenderoth, 2013). This is in contrast to the present results that reveal the Moho at a depth of 38-40 km along profile PQ2-004-005 (Fig. 5) and 38-42 km along profile PQ2-002 (Fig. 6). Our results show generally flat Moho with only minor shallowing toward the SW (Figs. 5, 6). The largest Moho depth gradient is shown in profile BGR16-212 (Fig. 10). In this case, the Moho is adopted from the earlier study by Janik et al. (2002). However, the Moho horizon is still deeper and flatter than in all the previous studies mentioned above. The Moho depth in our interpretation is comparable to that reported along the BABEL A seismic profile (BABEL Working Group, 1993). Nevertheless, the latter shows rougher morphology with a crustal keel beneath the STZ (BABEL Working Group, 1993; their figure 7).

The Moho horizon from the previous studies (e.g., Bleibinhaus et al., 1999; Krawczyk et al., 2002) roughly corresponds to the top of lower crust according to the present results (Figs. SM1-2). Consequently, all deeper reflectors represent in our interpretation reflective lower crust, a common feature of the continental lithosphere (e.g., Allmendinger et al., 1987; Mooney and Brocher, 1987; Reston, 1988; Holbrook et al., 1992). Therefore, we postulate that previously interpreted sub-Moho reflectors (Meissner and Krawczyk, 1999) actually belong to the lower crust or represent the Moho itself. Furthermore, the best pronounced lower crustal structures as well as local Moho perturbations are younger than previously believed (Meissner and Krawczyk, 1999) and were produced during the Late Cretaceous inversion (see below).

The deeper and flatter Moho along the presented seismic lines has several geological implications. Firstly, the relatively thick cratonic crust of the EEC continues to the very SW end of the studied profiles. Its thickness of c. 40 km corresponds to the average for the continental crust (Christensen and Mooney, 1995). This primarily concerns profiles PQ2-004-005 and PQ2-002 with relatively thin sedimentary cover (up to 4-6 km). Crustal thinning is more extensive along the SW section of profile BGR16-212 which transects the NW ending of the Mid-Polish Trough (Fig. 2). Secondly, there is an inverse correlation of the Moho depth and the thickness of sediments (depth to the basement) in sedimentary basins. This highlights the role of crustal-scale stretching in shaping the present-day lithospheric architecture. The sedimentary fill of sampled basins documents extension partitioned among three major events in early Paleozoic, Devonian-Carboniferous and Permian-Mesozoic. The amount of stretching increases from the NE to SW. Thirdly, the localized Moho perturbations are related to zones of crustal-scale thrusts produced in the course of the Late Cretaceous-early Paleogene inversion (see below). No features are detected that can possibly be associated with Proterozoic or Paleozoic tectonic sutures. The only uncertainty is related to the interpretation of profile BGR16-212 (Fig. 10). There is a Moho depth perturbation between km 110-150 of the profile of largely unknown origin (Janik et al., 2022). Furthermore, this zone partly overlaps with a middle crustal low-density body. The latter can be potentially replaced in gravity modelling by a crustal keel similar to that postulated for the profiles onshore Poland (Mazur et al., 2015, 2016b) and offshore in the Baltic Sea (BABEL Working Group, 1993; Makris and Wang, 1994).

5.2 Significance of the Sorgenfrei-Tornquist and Teisseyre-Tornquist Zones

The seismic interpretation and potential field modelling presented do not reveal any qualitative change in the character of crust along the studied profiles. This does not support concepts postulating a Proterozoic or Paleozoic tectonic suture coinciding with the TTZ (e.g., Franke, 1995; Dadlez et al., 2005). Consequently, the whole crustal section investigated seems to represent the EEC (former Baltica). Profile PQ2-004-005 shows the STZ as a zone of Late-Cretaceous-early Paleogene thick-skinned inversion both at the upper and lower crustal level (Fig. 5). This is consistent with earlier interpretation by BABEL Working Group (1991, 1993) who see the STZ as a "subversion zone", where inversion-related shortening is compensated by uplift of upper crust and thickening of lower crust. Furthermore, the STZ also coincides with the thickest sedimentary section intersected by the profile. Profile PQ2-002 shows the TTZ corresponding to the crystalline basement slope and the fragment of the sedimentary basin adjacent from the SW (Fig. 6). The zone also includes the SW part of the of the thick-skinned inversion zone. However, the latter extends much farther to the NE up to the Christiansø Block (Figs. 2, 3). PQ2-004 does not intersect the entire width of the TTZ that includes the NW termination of the Mid-Polish Trough. The latter observation is confirmed by profile BGR16-212 that cross-cut the whole TTZ (Figs. 2, 3). The TTZ coincides with the Mid-Polish Trough, the deepest part of the Permian-Mesozoic basin (Fig. 7). This is also a zone focusing the strongest Late-Cretaceous-early Paleogene inversion although its thick-skinned character is not confirmed due to shallow seismic imaging (Fig. 7). Summing up, the STZ and TTZ correspond to the localized zones of the Late Cretaceous-early Paleogene inversion. In the area directly south of Bornholm, intersected by profile PQ2-002, the pre-existing definition of the TTZ (e.g., Guterch et al., 1999, 2010) includes only this part of the inversion zone that involves the NW ending of the Mid-Polish Trough.

The observation reported above is in contrast with the interpretation of the TTZ as the Paleozoic suture zone (e.g., Franke, 1995; Dadlez et al., 2005; Narkiewicz et al., 2015) or the edge of the EEC (Guterch et al., 1986, 1999). This finding is also not fully consistent with the concept of the "Trans-European Suture Zone" – a broad and complex zone of Paleozoic terrane accretion between the TTZ and Variscan belt of Central Europe (Pharaoh, 1999). In contrast, the results obtained are in accordance with a critical reassessment of the Trans-European Fault by McCann and Krawczyk (2001). They are also close to the concept by Berthelsen (1998) postulating that the TTZ is the Permo-Mesozoic "pseudo-suture" developed during the opening of the Polish Basin. The TTZ was considered to have formed over a low-angle, listric décollement in the ductile part of the crust due to the early Permian continental rifting, according to the classical Wernicke model (1985). The difference compared to the Berthelsen's hypothesis is that the present study sees the TTZ as a feature formed due to inversion of the Permian-Mesozoic basin.

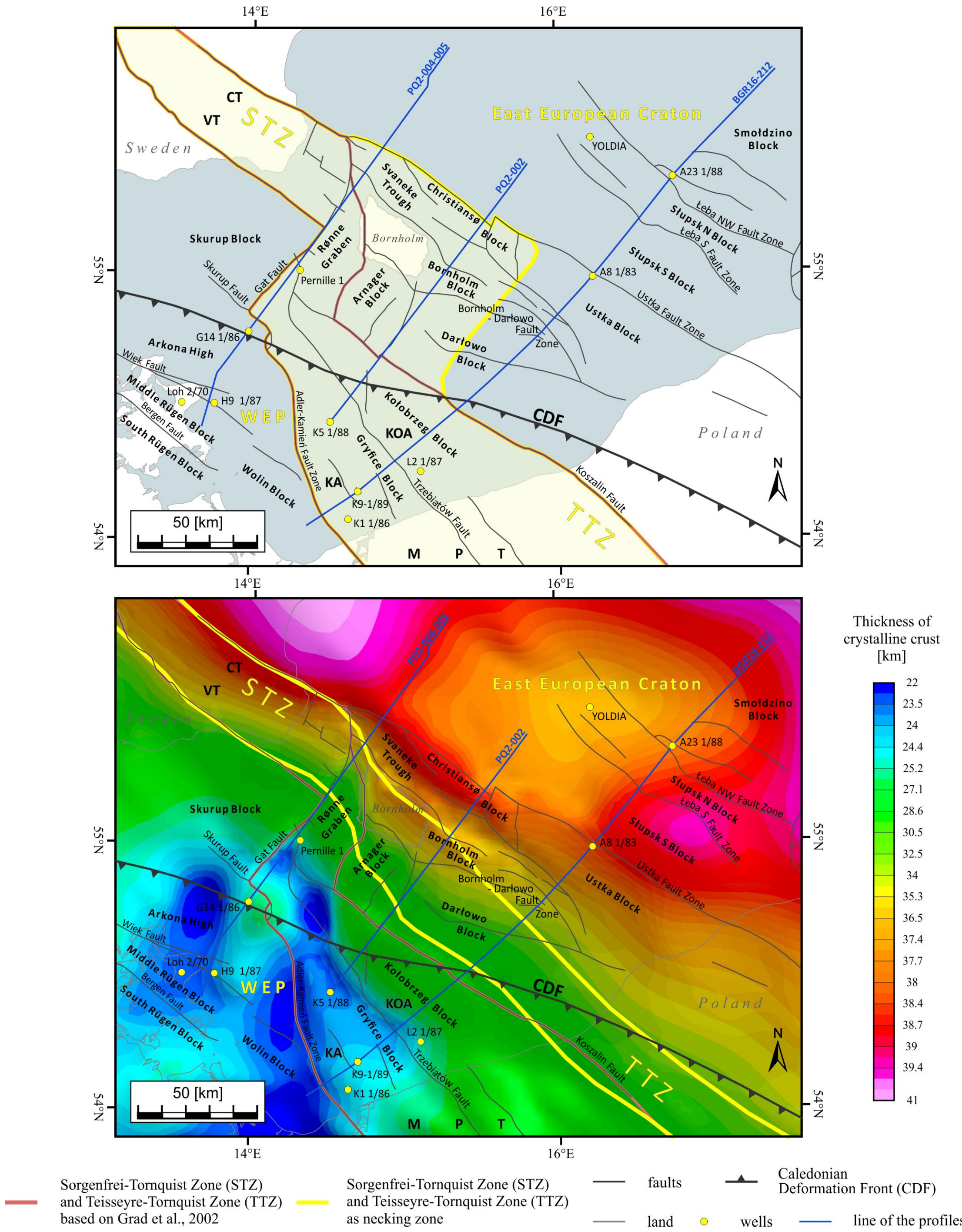

Figure 11. Two options of defining the Teisseyre-Tornquist and Sorgenfrei-Tornquist Zones (TTZ and STZ). (a) – zones of localized Late Cretaceous-early Paleogene thick-skinned inversion. (b) – a necking zone associated with polyphase crustal thinning, colorful grid shows thickness of crystalline crust (based on the Moho and top basement grids from Maystrenko and Scheck-Wenderoth, 2013). Brown lines depict classical extent of the TTZ and STZ (e.g., Pharaoh 1999; Grad et al., 2002; Siedel et al., 2018). Yellow lines show boundaries of the TTZ and STZ proposed in this paper. Abbreviations: CDF – Caledonian Deformation Front; CT –

Colonus Trough; KA – Kamień Anticline; KOA – Kołobrzeg Anticline; MPT – Mid-Polish Trough; STZ – Sorgenfrei-Tornquist Zone; TTZ – Teisseyre-Tornquist Zone; VT – Vomb Trough; WEP – West European Platform.

The TTZ was originally defined based on magnetic anomalies that are very strong in the Precambrian Platform due to the shallow crystalline basement, but largely attenuated farther SW by a thick sedimentary cover of the Mid-Polish Trough (Tornquist, 1908). Consequently, the TTZ has been for decades considered a fossil plate boundary of the EEC and the dividing line between old Precambrian and younger Paleozoic Europe (e.g., Tornquist 1908; Teisseyre 1921; Brochwicz-Lewiński et al., 1981; Pożaryski et al., 1982; Dadlez et al., 2005; Narkiewicz et al., 2015). With the advent of deep refraction sounding the TTZ was defined as a c. 50 km wide zone of Moho uplift by 6-8 km, but still representing the edge of the craton (Perchuć, 1984; Guterch et al., 1986, 1999). In later years, the termination of the EEC crust along the TTZ was questioned in some papers (Berthelsen, 1998; Pharaoh, 1999; Grad et al., 2002; Bayer et al., 2002; Malinowski et al., 2005; Żelaźniewicz et al., 2009; Mazur et al., 2015, 2016b). Mazur et al. (2016a) and Mikołajczak et al. (2019) redefined the TTZ as an Ediacaran crustal necking zone produced during the break-up of Rodinia. Nevertheless, the contribution of Permian-Mesozoic crustal stretching to attenuation of the EEC margin beneath the Polish Basin was also significant (Mazur et al., 2021). In the light of the present results, there are two possibilities of defining the TTZ and STZ. Firstly, to understand them as zones of Late Cretaceous-early Paleogene thick-skinned inversion. This would allow to retain a broad shape of the TTZ depicted in numerous papers (e.g., Grad et al., 2002) and the only correction required is including the area south of Bornholm, where the thick crystalline crust was inverted (Fig. 11a). The second possibility is to define the STZ and TTZ as an Ediacaran-Paleozoic necking zone associated with crustal thickness reduction (Fig. 11b). In this case, the TTZ is narrower and located in line with the STZ without a characteristic zig-zag along the Rønne Graben.

The seismic lines from the Baltic Sea indicate that the necking zone earlier postulated (Mikołajczak et al., 2019) is not only produced by Ediacaran rifting but had a polyphase origin comprising (1) late Ediacaran stretching related to break-up of Rodinia, (2) Devonian-Carboniferous extension of the Laurussia passive margin, and (3) early Permian continental rifting and later renewed extension in the Permian-Mesozoic Polish Basin. Out of these three events, the least explored is late Paleozoic pre-Permian continental rifting that resulted in over 3 km thick middle Devonian syn-rift and Late Devonian-early Carboniferous post-rift sediments SW of the TTZ (Fig. 7).

5.3 Mechanism of late Mesozoic basin inversion

Recent years have brought several accounts on the effects of Late Cretaceous-early Paleogene basin inversion in the southern Baltic Sea (Sopher et al., 2016; Al Hseinat and Hübscher, 2017; Ahlrichs et al., 2022; Pan et al., 2022; Krzywiec et al., 2022; Stachowska and Krzywiec, 2023). However, this study is the first to document the inversion structures at the scale of entire crust – from the Moho to base of the Cenozoic. Profiles PQ2-004-005 and PQ2-002 show a system of thrusts and backthrusts penetrating the entire crust in an 80-90 km wide inversion zone. Thrust faults are steepening upwards and appear as reverse faults in shallow crustal sections (Figs. 5, 6). The combination of thrusts and back-thrusts explains the position of hanging-walls of Cretaceous faults changing from the SW to NE (Figs. 5, 6). The footwalls host up to 1 km deep syn-inversion marginal troughs filled with Cretaceous sediments. No evidence is available for the Late Cretaceous reverse faults affecting older structures. Therefore, it is likely that the majority of inversion structures are newly formed in response to the Late Cretaceous compression. Similar mechanism of intra-cratonic inversion was postulated for Dnieper-Donbas Basin in eastern Ukraine, where a crustal-scale pop-up structure was formed (Maystrenko et al., 2003). The present study provides another example of thick-skinned inversion tectonics within the interior of the EEC. This confirms that horizontal compressional stress can be transferred far away from a collision zone and cause deformation at the scale of the entire crust. Rigid cratons are probably especially prone to this style of inversion since strain is not pervasively disseminated but localized in a relatively few zones of weakness.

Profiles PQ2-004-005 and BGR16-212 demonstrate that inversion was focused along the zones of thinned crust corresponding to pre-inversion weakness zones. They are represented by the Vomb and Colonus Troughs as well as the Mid-Polish Trough for the STZ and TTZ, respectively (Figs. 2, 3). However, both NW-SE oriented features are not located along one line, and they are linked by the Rønne Graben (Fig. 11a). Although the latter is also inverted the main inversion structures are not fully adjusted to its orientation. Especially, the STZ continues south of Bornholm into the area of thick crust with a relatively thin sedimentary cover (Figs. 2, 3, 6). A number of inversion-related faults and tectonic blocks exist there as the Darłowo, Bornholm and Christiansø Blocks (Figs. 2, 3). This situation implies a limited strike-slip component along the Rønne Graben during inversion. Conversely, the STZ was gradually dying out SE-ward of Bornholm as accommodation of shortening was overtaken by the TTZ.

The results of the present study are consistent with those obtained by Pan et al. (2022) in the STZ offshore Sweden. Their investigation revealed thrusts and pop-up structures developed along the inversion axis accompanied by subsidence troughs on its sides due to compressional deformation. Pan et al. (2022) interpreted the STZ as an intraplate foreland basin resulting from far-field NE-SW compression transmitted from the Africa-Iberia-Europe convergence zone. On the other hand, the current results do not fully support the previous interpretation by Deeks and Thomas (1995), who postulated an important role of dextral strike-slip displacement along the STZ and TTZ. We cannot exclude strike-slip displacements associated with inversion tectonics, but our data do not bring evidence in support of this idea. Furthermore, the continuation of STZ some distance SE of Bornholm argues against the interpretation of the Rønne Graben as a large-scale releasing bend in the dextral strike-slip system (Deeks and Thomas, 1995). Beyond this aspect, however, Deeks and Thomas's paper is one of the first to identify inversion tectonics in the southern Baltic Sea. Finally, BABEL Working Group (1991, 1993), Thybo et al. (1994) and Thybo (2000) were the first to advocate for thick-skinned inversion tectonics in the Baltic Sea with the STZ encompassing the inverted block of crystalline rocks near the surface and the crustal keel, imaged as a subdued Moho. The keel of low velocity and density was assumed to balance the weight of the crustal column beneath the elevated basement (Thybo, 2000).

6 Conclusions

The present study shows that the southern Baltic Sea is underlain by thick crust of the EEC. The Moho depth is in the range of 38-42 km slightly decreasing SE-ward. All deep reflectors represent in our interpretation reflective lower crust, a common feature of the continental lithosphere. Therefore, previously interpreted sub-Moho reflectors presumably belong to the lower crust.

The overall crustal architecture is mostly shaped by three phases of stretching in early Paleozoic, Devonian-Carboniferous, and Permian-Mesozoic that resulted in localized crustal thinning and growth of sedimentary basins. Out of these three events, the least explored is late Paleozoic pre-Permian continental rifting that resulted in over 3 km thick middle Devonian-early Carboniferous syn- to post-rift sediments.

The only Phanerozoic compressional event affecting the entire crust is Late Cretaceous-early Paleogene inversion induced by continental collision between Africa and Iberia. Inversion was mostly localized within the STZ and TTZ developed along the preexisting zones of crustal weakness – the Vomb and Colonus Troughs north of Bornholm (STZ) and the Mid-Polish Trough farther south (TTZ). Both STZ and TTZ include a system of thrusts and backthrusts penetrating the entire crust in an 80-90 km wide inversion zone, and forming a crustal-scale pop-up structure. The similar mechanism of intra-cratonic inversion was recognized for the Dnieper-Donbas Basin in eastern Ukraine, and it may be characteristic of rigid cratons where deformation is localized in a few zones of weakness. STZ and TTZ are not positioned in one line and, thus, the former is dying out SE-ward of Bornholm where accommodation of shortening is overtaken by the latter.

There is no evidence for Phanerozoic tectonic sutures or plate boundaries within the southern Baltic Sea. A crustal neck is situated directly NE of the Mid-Polish Trough and TTZ, but this feature results from polyphase crustal stretching. The Caledonian orogen is represented by a relatively thin orogenic wedge emplaced upon crystalline basement due to thin-skinned thrusting.

Acknowledgments

This study was supported by the Polish National Science Centre grant no. UMO-2017/27/B/ST10/02316. Cruise MSM52 has been funded by German Science Foundation DFG and Federal Ministry of Education and Research (BMBF). We thank Federal Institute for Geosciences and Natural Resources (BGR) for the license to use seismic data acquired during MSM52 cruise and their support during seismic data acquisition and sharing the data. Processing of the MSM52 seismic data was performed using Globe Claritas package under the academic license from Petrosys Ltd. We thank Manfred Stiller (GFZ Potsdam) for providing the processed PQ data. S. Stovba thanks the Polish National Science Centre for the grant UMO-2022/01/3/ST10/00030.

Open Research

The gravity and magnetic were licensed from Getech Group plc and are commercially available from the supplier. The ArcGIS project containing georeferenced images of the data and their derivatives is available at the repository of the Institute of Geological Sciences PAS (https://dataportal.ing.pan.pl). The same repository contains XField project with 2-D gravity and magnetic models as well as the seismic GeoGraphix project.

GeoGraphix software was used for seismic interpretation. Seismic data processing was performed using Globe Claritas package. 2-D gravity modelling was done using XField plugin to commercial version of OpendTect. The spatial data were compiled on ArcGIS platform version 10.3.

References

Ahlrichs, N., Noack, V., Hübscher, C., Seidel, E., Warwel, A., & Kley, J. (2022). Impact of Late Cretaceous inversion and Cenozoic extension on salt structure growth in the Baltic sector of the North German Basin. *Basin Research*, **34**(1), 220–250. https://doi.org/10.1111/bre.12617

Ahlrichs, N., Noack, V., Seidel, E. & Hübscher, C. (2023). Salt tectonics in intracontinental sedimentary basins: Triassic–Jurassic salt movement in the Baltic sector of the North German Basin and its relation to post-Permian regional tectonics. *Basin Research* **35**(4), 1433–1459. https://doi.org/10.1111/bre.12760

Al Hseinat, M., & Hübscher, C. (2017). Late Cretaceous to recent tectonic evolution of the North German Basin and the transition zone to the Baltic Shield/southwest Baltic Sea. *Tectonophysics*, **708**, 28–55. https://doi.org/10.1016/j.tecto.2017.04.021

Allmendinger, R.W., Nelson, K.D., Potter, C.J., Barazangi, M., Brown, L.D. & Oliver, J.T. (1987). Deep seismic reflection characteristics of the continental crust. *Geology*, **15**(4), 304–310. https://doi.org/10.1130/0091-7613(1987)15<304:DSRCOT>2.0.CO;2

ARK CLS, 2021. https://arkcls.com/software/xfield/. Accessed 06/12/2022.

BABEL Working Group (1991). Deep seismic survey images the structure of the Tornquist Zone beneath the Southern Baltic Sea. *Geophysical Research Letters*, **18**, 1091–1094. https://doi.org/10.1029/91GL00847

BABEL Working Group (1993). Deep seismic reflection/refraction interpretation of critical structure along BABEL profiles A and B in the southern Baltic Sea. *Geophysical Journal International*, **112**, 325–343. https://doi.org/10.1111/j.1365-246X.1993.tb01173.x

Babuška, V., & Plomerová, J. (2004). The Sorgenfrei–Tornquist Zone as the mantle edge of Baltica lithosphere: new evidence from three-dimensional seismic anisotropy. *Terra Nova*, **16**(5), 243–249. https://doi.org/10.1111/j.1365-3121.2004.00558.x

Bayer, U., Grad, M., Pharaoh, T.C., Thybo, H., Guterch, A., Banka, D., Lamarche, J., Lassen, A., Lewerenz, B., Scheck, M., & Marotta, A.M. (2002). The southern margin of the east European Craton: new results from seismic sounding and potential fields between the North Sea and Poland. *Tectonophysics*, **360**(1–4), 301–314. https://doi.org/10.1016/S0040-1951(02)00359-1

Berthelsen, A. (1992). Mobile Europe. In: Blundell, D., Freeman, R., Mueller, S. (Eds.), *The European Geotraverse: A Continent Revealed*. Cambridge University Press, Cambridge, pp. 153–164.

Berthelsen, A. (1998). The Tornquist Zone northwest of the Carpathians: an intraplatepseudosuture. *GFF*, **120**, 223–230. https://doi.org/10.1080/11035899801202223

Bleibinhaus, F., Beilecke, T., Bram, K., & Gebrande, H. (1999). A seismic velocity model for the SW Baltic Sea derived from BASIN'96 refraction seismic data. *Tectonophysics*, **314**, 269–283. https://doi.org/10.1016/S0040-1951(99)00248-6

Brocher, T.M. (2005). Empirical relations between elastic wave speeds and density in the Earth's crust. *Bulletin of the Seismological Society of America*, **95**(6), 2081–2092. https://doi.org/10.1785/0120050077

Brochwicz-Lewiński, W., Pożaryski, W., & Tomczyk, H. (1981). Wielkoskalowe ruchy przesuwcze wzdłuż SW brzegu platformy wschodnioeuropejskiej we wczesnym paleozoiku. *Przegląd Geologiczny*, **8**, 340, 385–396. [in Polish]

Central Geological Database, (2019). Polish Geological Institute. http://baza.pgi.gov.pl/. Accessed 18 Oct 2022.

Christensen, N.I., & Mooney, W.D. (1995). Seismic velocity structure and composition of the continental crust: A global view. *Journal of Geophysical Research: Solid Earth*, **100**(B6), 9761–9788. https://doi.org/10.1029/95JB00259

Cotte, N., Pedersen, H.A., & TOR Working Group (2002). Sharp contrast in lithospheric structure across the Sorgenfrei–Tornquist Zone as inferred by Rayleigh wave analysis of TOR1 project data. *Tectonophysics*, **360**(1-4), 75–88. https://doi.org/10.1016/S0040-1951(02)00348-7

Dadlez, R. (1993). Pre-Cainozoic tectonics of the southern Baltic Sea. *Geological Quarterly*, **37**(3), 431–450.

Dadlez, R. (2003). Mesozoic thickness pattern in the Mid-Polish Trough. Geological Quarterly, 47, 223–240.

Dadlez, R., Kowalczewski, Z., & Znosko, J. (1994). Some key problems of the pre-Permian tectonics of Poland. *Geological Quarterly*, **38**, 169–189.

Dadlez, R., Narkiewicz, M., Stephenson, R.A., Visser, M.T.M., & Van Wees, J.D. (1995). Tectonic evolution of the Mid-Polish Trough: modelling implications and significance for central European geology. *Tectonophysics*, **252**(1-4), 179–195. https://doi.org/10.1016/0040-1951(95)00104-2

Dadlez, R., Grad, M., & Guterch, A. (2005). Crustal structure below the Polish Basin: is it composed of proximal terranes derived from Baltica? *Tectonophysics*, **411**(1–4), 111–128. https://doi.org/10.1016/j.tecto.2005.09.004

Dallmeyer, R.D., Giese, U., Glasmacher, U., & Pickel, W. (1999). First 40Ar/39Ar age constraints for the Caledonian evolution of the Trans–European Suture Zone in NE Germany. Journal of the Geological Society, 156(2), 279–290. https://doi.org/10.1144/gsjgs.156.2.0279

Deeks, N.R., & Thomas, S.A. (1995). Basin inversion in strike-slip regime, the Tornquist Zone, Southern Baltic Sea. In: Buchanan, J.G., & Buchanan P.G. (Eds.), Basin Inversion. Geological Society Special Publication, 88, 319-338. https://doi.org/10.1144/GSL.SP.1995.088.01.18

DEKORP-BASIN Research Group (1998). Survey provides seismic insights into an old suture zone. *EOS*, **79**, 151–159. https://doi.org/10.1029/98EO00113

DEKORP-BASIN Research Group (1999). Deep crustal structure of the Northeast German basin: New DEKORP-BASIN '96 deep profiling results. *Geology*, **27**, 55–58. https://doi.org/10.1130/0091-7613(1999)027<0055:DCSOTN>2.3.CO;2

Erlström, M., Thomas, S.A., Deeks, N., & Sivhed, U. (1997). Structure and tectonic evolution of the Tornquist Zone and adjacent sedimentary basins in Scania and the southern Baltic Sea area. *Tectonophysics*, **271**(3-4), 191–215. https://doi.org/10.1016/S0040-1951(96)00247-8

EUGENO-S Working Group (1988). Crustal structure and tectonic evaluation of the transition between the Baltic Shield and the North German Caledonides (The EUGENO-S Project). *Tectonophysics*, **150**, 253–348. https://doi.org/10.1016/0040-1951(88)90073-X

Fletcher, K.M.U., Fairhead, J.D., Salem, A., Lei, K., Ayala, C., & Cabanillas, P.L.M. (2011). Building a higher resolution magnetic database for Europe for resource evaluation. *First Break*, **29**(4), 41–47. https://doi.org/0.3997/1365-2397.29.4.49508

Franke, D. (1995). The Caledonian terranes along the south-western border of the East European Platform—Evidence, speculation and open questions. In *The Trans-European Suture Zone:*

EUROPROBE in Libice 1993, Studia Geophysica et Geodaetica, **39**, Gee D.G., & Beckholmen, M., pp. 241–256.

Gossler, J., Kind, R., Sobolev, S.V., Kämpf, H., Wylegalla, K., Stiller, M., & TOR Working Group (1999). Major crustal features between the Harz Mountains and the Baltic Shield derived from receiver functions. *Tectonophysics*, **314**(1–3), 321–333. https://doi.org/10.1016/S0040-1951(99)00251-6

Grad, M., Guterch, A., & Mazur, S. (2002). Seismic refraction evidence for crustal structure in the central part of the Trans-European Suture Zone in Poland. In: Winchester, J.A., Pharaoh T.C., Verniers, J. (Eds.), *Palaeozoic Amalgamation of Central Europe*, Geological Society Special Publication, 201, Geological Society, London, pp. 295–309. https://doi.org/10.1144/GSL.SP.2002.201.01.14

Grad, M., & Polkowski, M. (2016). Seismic basement in Poland. *International Journal of Earth Sciences*, **105**(4), 1199–1214. https://doi.org/10.1007/s00531-015-1233-8

Grad, M., Tiira, T., & ESC Working Group (2009). The Moho depth map of the European Plate. *Geophysical Journal International*, **176**(1), 279–292. https://doi.org/10.1111/j.1365-246X.2008.03919.x

Graversen, O. (2004). Upper Triassic–Cretaceous stratigraphy and structural inversion offshore SW Bornholm, Tornquist Zone, Denmark. *Bulletin of the Geological Society of Denmark*, **51**, 111–136. https://doi.org/10.37570/bgsd-2004-51-08

Green, C.M., Fletcher, K.M.U., Cheyney, S., Dawson, G.J., & Campbell, S.J. (2019). Satellite gravity–enhancements from new satellites and new altimeter technology. *Geophysical Prospecting*, **67**(6-Geophysical Instrumentation and Acquisition), 1611–1619. https://doi.org/10.1111/1365-2478.12697

Guterch, A., & Grad, M. (2006). Lithospheric structure of the TESZ in Poland based on modern seismic experiments. *Geological Quarterly*, **50**(1), 23–32.

Guterch, A., Grad, M., Materzok, R., & Perchuć E., (1986). Deep structure of the Earth's crust in the contact zone of the Palaeozoic and Precambrian platforms in Poland (Tornquist-Teisseyre Zone). *Tectonophysics*, **128**(3), 251–279. https://doi.org/10.1016/0040-1951(86)90296-9

Guterch, A., Grad, M., Thybo, H., Keller, G.R., & the POLONAISE Working Group (1999). POLONAISE'97—An international seismic experiment between Precambrian and Variscan Europe in Poland. *Tectonophysics*, **314**(1–3), 101–121. https://doi.org/10.1016/S0040-1951(99)00239-5

Guterch, A., Wybraniec, S., Grad, M., Chadwick, R.A., Krawczyk, C.M., Ziegler, P.A., Thybo, H., & De Vos, W. (2010). Crustal structure and structural framework. In: Doornenbal, J.C., Stevenson, A.G. (Eds.), *Petroleum Geological Atlas of the Southern Permian Basin Area*. EAGE Publications, Houten, pp. 11–23.

Hansen, M., & Poulsen, V. (1977). *Ekskursionsfører nr. 1, Geologi på Bornholm*, VARV, København, 96 pp.

Hansen, D.L., Nielsen, S.B., & Lykke-Andersen, H. (2000). The post-Triassic evolution of the Sorgenfrei–Tornquist Zone—results from thermo-mechanical modelling. *Tectonophysics*, **328**(3-4), 245–267. https://doi.org/10.1016/S0040-1951(00)00216-X

Holbrook, W.S., Mooney, W.D., & Christensen, N.I. (1992). The seismic velocity structure of the deep continental crust. In: Fountain, D.M., Arculus R., & Kay R. (Eds.), *Continental Lower Crust*, Elsevier, Amsterdam, pp. 1–43.

Hübscher, C., Ahlrichs, H., Allum, G., Behrens, T., Bülow, J., Krawczyk, C., Damm, V., Demir, Ü., Engels, M., Frahm, L., Grzyb, G., Hahn, B., Heyde, I., Juhlin, C., Knevels, K., Lange, G., Bruun Lydersen, I., Malinowski, M., Noack, V., Preine, J., Rampersad, K., Schnabel, M., Seidel, E., Sopher, D., Stakemann, Jo. & Stakemann, Ja. (2017). BalTec - Cruise No. MSM52 – March 1 – March 28, 2016 – Rostock (Germany) – Kiel (Germany). MARIA S. MERIAN-Berichte, MSM52, 46 pp. DFGSenatskommission für Ozeanographie. https://doi.org/10.2312/cr_msm52

Janik, T., Wójcik, D., Ponikowska, M., Mazur, S., Skrzynik, T., Malinowski, M., & Hübscher, C. (2022). Crustal structure across the Teisseyre-Tornquist Zone offshore Poland based on a new refraction/wide-angle reflection profile and potential field modelling. *Tectonophysics*, **828**, 229271. https://doi.org/10.1016/j.tecto.2022.229271

Jaworowski, K., Wagner, R., Modliński, Z., Pokorski, J., Sokołowski, J., & Sokołowski, A. (2010). Marine ecogeology in semi-closed basin: case study on a threat of geogenic pollution of the southern Baltic Sea (Polish Exclusive Economic Zone). *Geological Quarterly*, **54**(2), 267–288.

Jóźwiak, W., Nowożyński, K., Mazur, S., & Jeż, M. (2022). Deep Electrical Resistivity Structure of the European Lithosphere in Poland Derived from 3-D Inversion of Magnetotelluric Data. *Surveys in Geophysics*, **43**, 1563–1586. https://doi.org/10.1007/s10712-022-09716-1

Katzung, G., Giese, U., Walter, R., & Von Winterfeld, C. (1993). The Rügen Caledonides, northeast Germany. *Geological Magazine*, **130**(5), 725–730. https://doi.org/10.1017/S0016756800021038

Kley, J. (2018). Timing and spatial patterns of Cretaceous and Cenozoic inversion in the Southern Permian Basin. In: Kilhams, B., Kukla, P.A., Mazur, S., Mckie, T., Mijnlieff, H.F., Van Ojik, K. (Eds.), *Mesozoic Resource Potential in the Southern Permian Basin*. Geological Society, London, Special Publications, **469**(1), 19–31. https://doi.org/10.1144/SP469.12

Kramarska, R., Krzywiec, P., Dadlez, R., Jegliński, W., Papiernik, B., Przezdziecki, P., & Zientara, P. (1999). *Geological map of the Baltic Sea bottom without Quaternary deposits, 1: 500 000*. Państwowy Instytut Geologiczny, Gdańsk-Warszawa.

Krawczyk, C.M., Stiller, M., & DEKORP-BASIN Research Group (1999). Reflection seismic constraints on Paleozoic crustal structure and Moho beneath the NE German Basin. *Tectonophysics*, **314**, 241–253. https://doi.org/10.1016/S0040-1951(99)00246-2

Krawczyk, C.M., Eilts, F., Lassen, A., & Thybo, H. (2002). Seismic evidence of Caledonian deformed crust and uppermost mantle structures in the northern part of the Trans-European Suture Zone, SW Baltic Sea. *Tectonophysics*, **360**(1-4), 215–244. https://doi.org/10.1016/S0040-1951(02)00355-4

Krzywiec, P. (2002). Mid-Polish Trough inversion – seismic examples, main mechanisms and its relationship to the Alpine–Carpathian collision. *EGU Stephan Mueller Special Publication Series*, **1**, 151–165.

Krzywiec, P., Kramarska, R., & Zientara, P. (2003). Strike-slip tectonics within the SW Baltic Sea and its relationship to the inversion of the Mid-Polish Trough – evidence from high-resolution seismic data. *Tectonophysics*, **373**(1-4), 93–105. https://doi.org/10.1016/S0040-1951(03)00286-5

Krzywiec, P. (2006a). Triassic - Jurassic evolution of the Pomeranian segment of the Mid-Polish Trough – basement tectonics and sedimentary patterns. *Geological* Quarterly, **51**(1), 139–150.

Krzywiec, P. (2006b). Structural inversion of the Pomeranian and Kuiavian segments of the Mid-Polish Trough – lateral variations in timing and structural style. *Geological Quarterly*, **51**(1), 151–168.

Krzywiec, P., Kufrasa, M., Poprawa, P., Mazur, S., Koperska, M., & Ślemp, P. (2022). Together but separate: decoupled Variscan (late Carboniferous) and Alpine (Late Cretaceous–Paleogene) inversion tectonics in NW Poland. *Solid Earth*, **13**(3), 639–658. https://doi.org/10.5194/se-13-639-2022

Lassen, N.A., Thybo, H., & Berthelsen, A. (2001). Reflection seismic evidence for Caledonian deformed sediments above Sveconorwegian basement in the southwestern Baltic Sea. *Tectonics*, **20**(2), 268–276. https://doi.org/10.1029/2000TC900028

Liboriussen, J., Ashton, P., & Tygesen, T. (1987). The tectonic evolution of the Fennoscandian Border Zone in Denmark. *Tectonophysics*, **137**, 21–29. https://doi.org/10.1016/0040-1951(87)90310-6

Ludwig, W.J., Nafe, J.E., & Drake, C.L. (1970). Seismic refraction. In Maxwell, A.E. (Ed.), *The Sea*, vol. 4. Wiley-Interscience, New York, pp. 53–84.

Makris, J., & Wang, S.-R. (1994). Crustal Structure at the Tornquist-Teisseyre zone in the Southern Baltic Sea. *Zeitschrift für Geologische Wissenschaften*, **22**(1/2), 47–54.

Malinowski, M., Żelaźniewicz, A., Grad, M., Guterch, A., Janik, T., & Celebration Working Group (2005). Seismic and geological structure of the crust in the transition from Baltica to

Palaeozoic Europe in SE Poland – CELEBRATION 2000 experiment, profile CEL02. *Tectonophysics*, **401**(1), 55–77. https://doi.org/10.1016/j.tecto.2005.03.011

Maystrenko, Y.P., & Scheck-Wenderoth, M. (2013). 3D lithosphere-scale density model of the central European Basin System and adjacent areas. *Tectonophysics*, **601**, 53–77. https://doi.org/10.1016/j.tecto.2013.04.023

Maystrenko, Y., Stovba, S., Stephenson, R., Bayer, U., Menyoli, E., Gajewski, D., Hübscher, C., Rabbel, W., Saintot, A., Starostenko, V., & Thybo, H. (2003). Crustal-scale pop-up structure in cratonic lithosphere: DOBRE deep seismic reflection study of the Donbas fold belt, Ukraine. *Geology*, **31**(8), 733–736. https://doi.org/10.1130/G19329.1

Maystrenko, Y., Bayer, U., & Scheck-Wenderoth, M. (2005). The Glueckstadt Graben, a sedimentary record between the North and Baltic Sea in north Central Europe. *Tectonophysics*, **397**(1-2), 113–126. https://doi.org/10.1016/j.tecto.2004.10.004

Maystrenko, Y., Bayer, U., Brink, H.-J., & Littke, R. (2008). The central European Basin System – An Overview. In: Littke, R., Bayer, U., Gajewski, D., Nelskamp, S. (Eds.), *Dynamics of Complex Sedimentary Basins. The Example of the Central European Basin System.* Springer-Verlag, Berlin-Heidelberg, pp. 15–34. https://doi.org/10.1007/978-3-540-85085-4_2

Mazur, S., Scheck-Wenderoth, M., & Krzywiec, P. (2005). Different modes of the Late Cretaceous–Early Tertiary inversion in the North German and Polish basins. *International Journal of Earth Sciences*, **94**, 782–798. https://doi.org/10.1007/s00531-005-0016-z

Mazur, S., Mikolajczak, M., Krzywiec, P., Malinowski, M., Buffenmyer, V., & Lewandowski, M. (2015). Is the Teisseyre-Tornquist Zone an ancient plate boundary of Baltica? *Tectonics*, **34**, 2465–2477. https://doi.org/10.1002/2015TC003934

Mazur, S., Mikołajczak, M., Krzywiec, P., Malinowski, M., Buffenmyer, V., & Lewandowski, M. (2016a). Reply to Comment by M Narkiewicz and Z Petecki on “Is the Teisseyre-Tornquist Zone an ancient plate boundary of Baltica?”. *Tectonics*, **35**(6), 1600–1607. https://doi.org/10.1002/2016TC004127

Mazur, S., Mikolajczak, M., Krzywiec, P., Malinowski, M., Lewandowski, M., & Buffenmyer, V. (2016b). Pomeranian Caledonides, NW Poland–a collisional suture or thin-skinned fold-and-thrust belt? *Tectonophysics*, **692**, 29–43. https://doi.org/10.1016/j.tecto.2016.06.017

Mazur, S., Porębski, S. J., Kędzior, A., Paszkowski, M., Podhalańska, T., & Poprawa, P. (2018). Refined timing and kinematics for Baltica–Avalonia convergence based on the sedimentary record of a foreland basin. *Terra Nova*, **30**(1), 8–16. https://doi.org/10.1111/ter.12302

Mazur, S., Malinowski, M., Maystrenko, Y.P., & Gągała, Ł. (2021). Pre-existing lithospheric weak zone and its impact on continental rifting–The Mid-Polish Trough, Central European

Basin System. *Global and Planetary Change*, **198**, 103417. https://doi.org/10.1016/j.gloplacha.2021.103417

MacLeod, I.N., Jones, K., & Dai, T.F. (1993). 3-D analytic signal in the interpretation of total magnetic fi eld data at low magnetic latitudes. *Exploration Geophysics*, **24**, 679–691. https://doi.org/10.1071/EG993679

McCann, T. (1996). Pre-Permian of the north-east German Basin. *Geological Journal*, **31**(2), 159–177. https://doi.org/10.1002/(SICI)1099-1034(199606)31:2<159::AID-GJ705>3.0.CO;2-8

McCann, T., & Krawczyk, C.M. (2001). The Trans-European fault: a critical reassessment. *Geological Magazine*, **138**(1), 19–29. https://doi.org/10.1017/S0016756801004915

McCann, T., Pascal, C., Timmerman, M.J., Krzywiec, P., López-Gómez, J., Wetzel, L., Krawczyk, C.M., Rieke, H., & Lamarche, J. (2006). Post-Variscan (end Carboniferous-Early Permian) basin evolution in western and central Europe. Geological Society, London, Memoirs, 32(1), pp. 355–388. https://doi.org/10.1144/GSL.MEM.2006.032.01.22

Meissner, R., & Krawczyk, C.M. (1999). Caledonian and Proterozoic terrane accretion in the South-West Baltic Sea. *Tectonophysics*, **314**(1–3), 255–267. https://doi.org/10.1016/S0040-1951(99)00247-4

Mężyk, M., Malinowski, M., & Mazur, S., 2019. Imaging the East European Craton margin in northern Poland using extended correlation processing of regional seismic reflection profiles. *Solid Earth*, **10**(3), 683–696. https://doi.org/10.5194/se-10-683-2019

Mikołajczak, M., Mazur, S., & Gągała, Ł. (2019). Depth-to-basement for the east European Craton and Teisseyre-Tornquist Zone in Poland based on potential field data. *International Journal of Earth Sciences*, **108**(2), 547–567. https://doi.org/10.1007/s00531-018-1668-9

Modliński, Z., & Podhalańska, T. (2010). Outline of the lithology and depositional features of the lower Paleozoic strata in the Polish part of the Baltic region. *Geological Quarterly*, **54**(2), 109–121.

Mogensen, T.E. (1994). Palaeozoic structural development along the Tornquist Zone, Kattegat area, Denmark. *Tectonophysics*, **240**, 191–214. https://doi.org/10.1016/0040-1951(94)90272-0

Mooney, W.D., & Brocher, T.M. (1987). Coincident seismic reflection/refraction studies of the continental lithosphere: a global review. *Geophysical Journal International*, **89**(1), 1–6. https://doi.org/10.1111/j.1365-246X.1987.tb04379.x

Narkiewicz, M., Maksym, A., Malinowski, M., Grad, M., Guterch, A., Petecki, Z., Probulski, J., Janik, T., Majdański, M., Środa, P., Czuba, W., Gaczyński, E., & Jankowski, L. (2015). Transcurrent nature of the Teisseyre–Tornquist Zone in Central Europe: results of the

POLCRUST-01 deep reflection seismic profile. *International Journal of Earth Sciences*, **104**(3), 775–796. https://doi.org/10.1007/s00531-014-1116-4

Narkiewicz, M., & Petecki, Z. (2017). Basement structure of the Paleozoic Platform in Poland. *Geological Quarterly*, **61**(2), 502–520.

Nguyen, Q., Malinowski, M., Kramarska, R., Kaulbarsz, D., Mil, L., & Hübscher, C. (2023). Gas-Escape features along the Trzebiatów fault offshore Poland: Evidence for a leaking petroleum system. *Marine and Petroleum Geology*, **156**, 106431. https://doi.org/10.1016/j.marpetgeo.2023.106431

Pan, Y., Seidel, E., Juhlin, C., Hübscher, C., & Sopher, D. (2022). Inversion tectonics in the Sorgenfrei–Tornquist Zone: insight from new marine seismic data at the Bornholm Gat, SW Baltic Sea. *GFF*, **144**(2), 71–88. https://doi.org/10.1080/11035897.2022.2071335

Perchuć, E. (1984). Structure of the Earth's crust in Southestern Poland. In: Symposium on Geodynamics. Jabłonna, 13–15 April 1981, *Publications of the Institute of Geophysics, Polish Academy of Sciences*, **160**, A-13, Państwowe Wydawnictwo Naukowe, Warszawa – Łódź, pp. 77–86.

Petecki, Z. (2002). Gravity and magnetic modelling along the seismic LT-7 profile. *Przegląd Geologiczny*, **50**, 630–633 (in Polish, English summary).

Pharaoh, T.C. (1999). Palaeozoic terranes and their lithospheric boundaries within the Trans-European Suture Zone (TESZ): a review. *Tectonophysics*, **314**(1), 17–41. https://doi.org/10.1016/S0040-1951(99)00235-8

Pharaoh, T.C., Winchester, J.A., Verniers, J., Lassen, A., & Seghedi, A. (2006). The western accretionary margin of the East European Craton: an overview. In: Gee, D.G., & Stephenson, R.A. (Eds.), *European Lithosphere Dynamics*. Geological Society of London Memoirs, **32**, pp. 291–311.

Piske, J., Rasch, H.-J., Neumann, E., & Zagora, K. (1994). Geologischer Bau und Entwicklung des Präperms der Insel Rügen und des angrenzenden Seegebietes. *Zeitschrift der Deutschen Gesellschaft*, **22**(1/2), 212–226.

Pokorski, J. (2010). Geological section through the lower Paleozoic strata of the Polish part of the Baltic region. *Geological Quarterly*, **54**(2), 123–130.

Poprawa, P. (2019). Geological setting and Ediacaran–Palaeozoic evolution of the western slope of the East European Craton and adjacent regions. *Annales Societatis Geologorum Poloniae*, **89**, 347−380. https://doi.org/10.14241/asgp.2019.23

Poprawa, P., Šliaupa, S., Stephenson, R., & Lazauskien, J. (1999). Late Vendian–Early Palaeozoic tectonic evolution of the Baltic Basin: regional tectonic implications from subsidence analysis. *Tectonophysics*, **314**(1), 219–239. https://doi.org/10.1016/S0040-1951(99)00245-0

Pożaryski, W., Brochwicz-Lewiński, W., & Tomczyk, H. (1982). O heterochroniczności linii Teisseyre'a-Tornquista. *Przegląd Geologiczny*, **11**, 355, 569–574. [in Polish]

Reston, T.J. (1988). Evidence for shear zones in the lower crust offshore Britain. *Tectonics*, **7**(5), 929–945. https://doi.org/10.1029/TC007i005p00929

Scheck-Wenderoth, M., Krzywiec, P., Zühlke, R., Maystrenko, Y., & Froitzheim, N. (2008). Permian to Cretaceous tectonics, In: McCann (Ed.), *The Geology of Central Europe Volume 2: Mesozoic and Cenozoic*, Geological Society of London, pp. 999–1030. https://doi.org/10.1144/CEV2P.4

Schlüter, H.U., Jürgens, U., Binot, F., & Best, G. (1998). The importance of geological structures as natural sources of potentially hazardous substances in the southern part of the Baltic Sea. *Zeitschrift der Deutschen Geologischen Gesellschaft*, **44**(1), 26–32.

Seidel, E., Meschede, M., & Obst, K. (2018). The Wiek Fault System east of Rügen Island: origin, tectonic phases and its relationship to the Trans-European Suture Zone. Mesozoic Resource Potential in the Southern Permian Basin. In: Kilhams, B., Kukla, P.A., Mazur, S., McKie, T., Mijnlieff, H.F., & van Ojik K. (Eds.), *Mesozoic Resource Potential in the Southern Permian Basin*. Geological Society, London, Special Publications, **469**(1), pp. 59–82. https://doi.org/10.1144/SP469.10

Smit, J., van Wees, J.D., & Cloetingh, S. (2016). The Thor suture zone: from subduction to intraplate basin setting. *Geology*, **44**, 707–710. https://doi.org/10.1130/G37958.1

Smit, J., van Wees, J.D., & Cloetingh, S. (2018). Early Carboniferous extension in East Avalonia: 350 my record of lithospheric memory. *Marine and Petroleum Geology*, **92**, 1010–1027. https://doi.org/10.1016/j.marpetgeo.2018.01.004

Sopher, D., Erlström, M., Bell, N., & Juhlin, C. (2016). The structure and stratigraphy of the sedimentary succession in the Swedish sector of the Baltic Basin: New insights from vintage 2D marine seismic data. *Tectonophysics*, **676**, 90–111. https://doi.org/10.1016/j.tecto.2016.03.012

Stachowska, A., & Krzywiec, P. (2023). The Late Cretaceous tectono-sedimentary evolution of northern Poland–A seismic perspective on the role of transverse and axial depositional systems during basin inversion. *Marine and Petroleum Geology*, **152**, 106224. https://doi.org/10.1016/j.marpetgeo.2023.106224

Stephenson, R., Schiffer, C., Peace, A., Nielsen, S.B., & Jess, S. (2020). Late Cretaceous-Cenozoic basin inversion and palaeostress fields in the North Atlantic-western Alpine-Tethys realm: Implications for intraplate tectonics. *Earth-Science Reviews*, **210**, 103252. https://doi.org/10.1016/j.earscirev.2020.103252

Talwani, M., & Ewing, M. (1960). Rapid computation of gravitational attraction of three-dimensional bodies of arbitrary shape. *Geophysics*, **25**, 203–225. https://doi.org/10.1190/1.1438687

Tanner, B., & Meissner, R. (1996). Caledonian deformation upon southwest Baltica and its tectonic implications: alternatives and consequences. *Tectonics*, **15**(4), 803–812. https://doi.org/10.1029/95TC03686

Teisseyre, W. (1921). O stosunku wewnętrznych brzegów zapadlin przedkarpackich do krawędzi fliszu karpackiego. *Sprawozdania Polskiego Instytutu Geologicznego*, **I** (2, 3), 103–138. [in Polish]

Tesauro, M., Kaban, M.K., & Cloetingh, S.A. (2008). EuCRUST-07: A new reference model for the European crust. *Geophysical Research Letters*, **35**(5). https://doi.org/10.1029/2007GL032244

Thybo, H. (2000). Crustal structure and tectonic evolution of the Tornquist Fan region as revealed by geophysical methods. *Bulletin of Geological Society of Denmark*, **46**, 145–160.

Thybo, H., Abramovitz, T., Lassen, A., & Schjøth, F. (1994). Deep structure of the Sorgenfrei-Tornquist zone interpreted from BABEL seismic data. *Zeitschrift für Geologische Wissenschaften*, **22**, 3–17.

Thybo, H. (2001). Crustal structure along the EGT profile across the Tornquist Fan interpreted from seismic, gravity and magnetic data. *Tectonophysics*, **334**(3-4), 155–190. https://doi.org/10.1016/S0040-1951(01)00055-5

Tornquist, A. (1908). Die Feststellung des Sudwesttrendes des baltich-russisschen Schiedes und die geotektonische Zugehorigheit der ost-preussischen Scholle. *Schriften der Physikalisch-Oekonomischen Gesellschaft zu Königsberg*, **49**, 1, 1–12.

van Wees, J. D., Stephenson, R. A., Ziegler, P. A., Bayer, U., McCann, T., Dadlez, R., Gaupp, R., Narkiewicz, M., Bitzer, F., & Scheck, M. (2000). On the origin of the Southern Permian Basin, Central Europe. *Marine and Petroleum Geology*, **17**, 43–59. https://doi.org/10.1016/S0264-8172(99)00052-5

Vejbæk, O.V. (1997). Dybe strukturer i danske bassiner. Geologisk Tidsskrift 4, 1–31.

Vejbæk, O.V., Stouge, S., & Poulsen, K.D. (1994). Palaeozoic tectonic and sedimentary evolution and hydrocarbon prospectivity in the Bomholm area. *Danmarks Geologiske Undersøgelse*, **A34**, 1–23.

Wernicke, B. (1985). Uniform-sense normal simple shear of the continental lithosphere. *Canadian Journal of Earth Sciences*, **22**(1), 108–125. https://doi.org/10.1139/e85-009

Yegorova, T., Bayer, U., Thybo, H., Maystrenko, Y., Scheck-Wenderoth, M., & Lyngsie, S.B. (2007). Gravity signals from the lithosphere in the Central European Basin System. *Tectonophysics*, **429**(1-2), 133–163. https://doi.org/10.1016/j.tecto.2006.10.002

Żelaźniewicz, A., Buła, Z., Fanning, M., Seghedi, A. & Żaba, J. (2009). More evidence on Neoproterozoic terranes in Southern Poland and southeastern Romania. *Geological Quarterly*, **53**(1), 93–124.

Ziegler, P.A., & Dèzes, P. (2006). Crustal evolution of western and central Europe. *Geological Society, London, Memoirs*, **32**(1), pp. 43–56. https://doi.org/10.1144/GSL.MEM.2006.032.01.03

Captions for figures and tables

Figure 1. Location of the BGR16-212, DEKORP-PQ (PQ2-004-005 and PQ2-002) and other seismic profiles: BABEL A (BABEL Working Group, 1991, 1993), TTZ'92/II (Makris and Wang, 1994) and PolandSPAN^{TM} PL-5400 and PL-5600 (Mazur et al., 2015, 2016b) on the background of a simplified tectonic map of the transition zone from the East European Craton to West European Platform. Yellow points refer to the location of offshore boreholes (Erlström et al., 1997; Sopher et al., 2016; Central Geological Database, 2019). Location of the Teisseyre-Tornquist Zone and Sorgenfrei-Tornquist Zones after Grad et al. (2002). Abbreviations: CDF – Caledonian Deformation Front; EA – East Avalonia; STZ – Sorgenfrei-Tornquist Zone; TTZ – Teisseyre-Tornquist Zone; VF – Variscan Front. The coordinate system of this and next figures is WGS 1984 UTM Zone 33 N.

Figure 2. Geological map of the southern Baltic Sea without post-Paleocene sediments after Kramarska et al. (1999), Schlüter et al. (1998), Sopher et al. (2016) and Pre-Quaternary map of Bornholm (Hansen and Poulsen, 1977). Position of main faults and tectonic blocks as well as the Teisseyre-Tornquist and Sorgenfrei-Tornquist Zones are adapted from Seidel et al. (2018). The studied seismic profiles are shown as blue lines. Abbreviations: CT – Colonus Trough; KA – Kamień Anticline; KOA – Kołobrzeg Anticline; MPT – Mid-Polish Trough; STZ – Sorgenfrei-Tornquist Zone; TTZ – Teisseyre-Tornquist Zone; VT – Vomb Trough; WEP – West European Platform.

Figure 3. Tectonic map of the southern Baltic Sea. Position of main faults and tectonic blocks are based on Kramarska et al. (1999), Krzywiec et al. (2003), Jaworowski et al. (2010), Pokorski et al. (2010) and Seidel et al. (2018). Location of the STZ and TTZ is modified from Grad et al. (2002). Yellow points refer to the location of offshore boreholes (Erlström et al., 1997; Sopher et al., 2016; Central Geological Database, 2022). Abbreviations: CDF – Caledonian Deformation Front; CT – Colonus Trough; KA – Kamień Anticline; KOA – Kołobrzeg Anticline; MPT – Mid-Polish Trough; STZ – Sorgenfrei-Tornquist Zone; TTZ – Teisseyre-Tornquist Zone; VT – Vomb Trough; WEP – West European Platform.

Figure 4. Gravity and magnetic anomaly maps. Location of main faults and tectonic blocks (modified from Seidel et al., 2018) overlaid on the Free Air gravity (a) and Reduced-to-Pole magnetic (b) anomaly maps. Position of the BGR16-212, PQ2-004-005, PQ2-002 profiles and boreholes is indicated. Gravity and magnetic data provided by Getech Group plc.

Figure 5. Seismic interpretation of the PQ2-004-005 profile. Vertical exaggerations are 7:1 for the upper part of the profile, and 1:1 for the full profile. CDF – Caledonian Deformation Front, STZ – Sorgenfrei-Tornquist Zone. Uninterpreted upper 7 km are shown in Figure SM1.

Figure 6. Seismic interpretation of the PQ2-002 profile. Vertical exaggerations are 6.2:1 for the upper part of the profile, and 1:1 for the full profile. CDF – Caledonian Deformation Front, TTZ – Teisseyre-Tornquist Zone. Uninterpreted upper 6 km are shown in Figure SM1.

Figure 7. Seismic interpretation of the BGR16-212 profile. Vertical exaggeration is 7:1. CDF – Caledonian Deformation Front, TTZ – Teisseyre-Tornquist Zone. Uninterpreted data are shown in Figure SM1.

Figure 8. Two-dimensional gravity and magnetic model for the PQ2-004-005 profile. (a, b) – gravity and magnetic data, respectively. Green, dotted lines – observed and green, solid lines – modelled. Grey, dashed line shows the magnitude of error. (c) – vertically exaggerated (7:1) upper part of the geological model. (d) – vertically exaggerated (1:1) full geological model based on the seismic profile. Numbers indicate densities (D) in g/cm^3 and susceptibilities (S) in SI convention. Abbreviations: CDF – Caledonian Deformation Front; STZ – Sorgenfrei-Tornquist Zone.

Figure 9. Two-dimensional gravity and magnetic model for the PQ2-002 profile. (a, b) – gravity and magnetic data, respectively. Green, dotted lines – observed and green, solid lines – modelled. Grey, dashed line shows the magnitude of error. (c) – vertically exaggerated (9:1) upper part of the geological model. (d) – vertically exaggerated (1:1) full geological model based on the seismic profile. Numbers indicate densities (D) in g/cm^3 and susceptibilities (S) in SI convention. Abbreviations: CDF – Caledonian Deformation Front; TTZ – Teisseyre-Tornquist Zone.

Figure 10. Two-dimensional gravity and magnetic model for the BGR16-212 profile. (a, b) – gravity and magnetic data, respectively. Green, dotted lines – observed and green, solid lines – modelled. Grey, dashed line shows the magnitude of error. (c) – vertically exaggerated (7:1) upper part of the geological model. (d) – vertically exaggerated (1.5:1) full geological model based on the seismic profile. Thick red line in (d) represents the top of crystalline basement. Numbers indicate densities (D) in g/cm^3 and susceptibilities (S) in SI convention. Abbreviations: CDF – Caledonian Deformation Front; TTZ – Teisseyre-Tornquist Zone.

Figure 11. Two options of defining the Teisseyre-Tornquist and Sorgenfrei-Tornquist Zones (TTZ and STZ). (a) – zones of localized Late Cretaceous-early Paleogene thick-skinned inversion. (b) – a necking zone associated with polyphase crustal thinning, colorful grid shows thickness of crystalline crust (based on the Moho and top basement grids from Maystrenko and Scheck-Wenderoth, 2013). Brown lines depict classical extent of the TTZ and STZ (e.g., Pharaoh 1999; Grad et al., 2002; Siedel et al., 2018). Yellow lines show boundaries of the TTZ and STZ proposed in this paper. Abbreviations: CDF – Caledonian Deformation Front; CT – Colonus Trough; KA – Kamień Anticline; KOA – Kołobrzeg Anticline; MPT – Mid-Polish Trough; STZ – Sorgenfrei-Tornquist Zone; TTZ – Teisseyre-Tornquist Zone; VT – Vomb Trough; WEP – West European Platform.

Table 1. Synopsis of tectonic events in the area of the southern Baltic Sea.

Table 2. Acquisition parameters of the DEKORP-BASIN’96 PQ2 and BalTec reflection seismic profiles.

Table 3. Key for density and susceptibility values used in the modelling of profiles PQ2-002, PQ2-004-005 and BGR16-212.

Supplementary Materials:

SM1 – Uninterpreted seismic data for upper parts of seismic profiles.

SM2 – Alternative gravity and magnetic models for profile PQ-004-005.

SM3 – Alternative gravity and magnetic models for profile PQ-002.

SM4 – Alternative gravity and magnetic models for profile BGR16-212.

SM5 – Gravity and magnetic model for profile BGR16-212 without a low-density body.